journal of the international meteor organization

WGN

41:6
december 2013

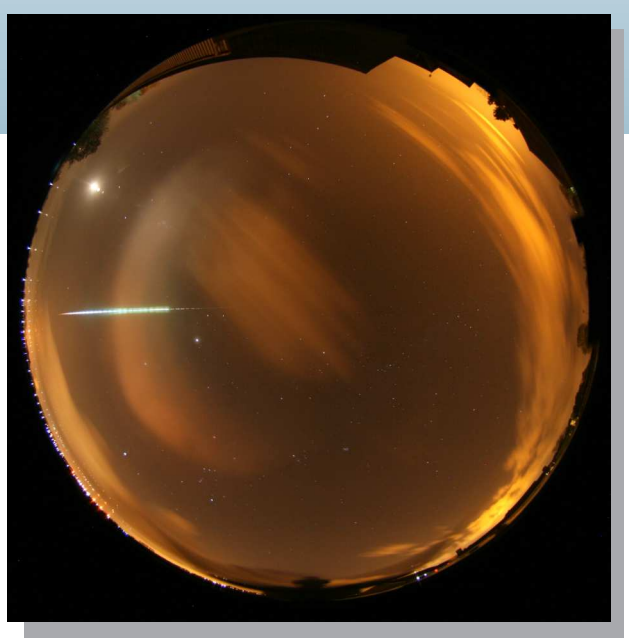

Solar longitudes 2014
General relativistic orbital precession
2013 η-Aquariid outburst results
The UK fireball of 2013 March 30
August–September video meteors
Meteor Beliefs Project decennial

ISSN 1016-3115

WGN Vol. 41, No. 6, December 2013, pp. 177 – 216

Administrative

Meteor science

Preliminary results

History

Front cover photo

A magnitude −10 fireball captured on 2013 October 30 at $03^{h}35^{m}$ UT by the EN95 Benningbrooek all-sky station. Photo courtesy: Jos Nijland. See the back cover for more records of the same fireball.

Writing for WGN

This Journal welcomes papers submitted for publication. All papers are reviewed for scientific content, and edited for English and style. Instructions for authors can be found in WGN **31:4**, 124–128, and at `http://www.imo.net/docs/writingforwgn.pdf` .

Cover design

Rainer Arlt

Legal address

International Meteor Organization, Jozef Mattheessensstraat 60, 2540 Hove, Belgium.

First announcement of the International Meteor Conference 2014

Paul Roggemans

The 2014 International Meteor Conference will take place in Giron, France, a nice village in the French Jura. This conference will be organized by the French meteor team of IMCCE assisted by amateur meteor workers and will take place from 2014 September 18–21. Giron is at 60 km from Geneva, 110 km from Lyon and 500 km from Paris (Figure 1). Giron can be easily reached by car via highway A40 (E21–E62), via exit St Germain de Joux, 9 km from Giron. The nearest high speed train station is at 20 km while many flight destinations are available at the airports of Geneva, Lyon, Marseille and Paris.

A shuttle will be organized to pick up participants from the nearest train station.

The IMC will be organized in the "Chalet de la Fauconière" where a suitable lecture room, a dining room for 150 persons and 120 beds are available in shared rooms (3 to 6 persons), a typical youth accommodation. People who prefer more privacy and comfort can chose between a single and a double room in the "Centre Montagnard" which is at 1 km distance from the IMC host at Fauconière.

The IMC excursion will bring us to the CERN facilities close to Geneva in Switzerland.

The standard IMC fee for 2014 will be 170 Euro per person including full board (3 nights with breakfasts, lunches and dinners), an IMC T-shirt, the IMC excursion and a copy of the 2014 IMC Proceedings. Accommodation in a double room is offered for a supplement of 25 Euro and a single room for a supplement of 50 Euro.

More information will be made soon available via `http://www.imo.net/imc2014`. The IMC organizers can be contacted via `imc2014@imo.net`. We expect this third IMC in France to be similar in style like the enjoyable previous IMC's in France which took place in June 2007 in Barèges and in September 1993 in Puimichel.

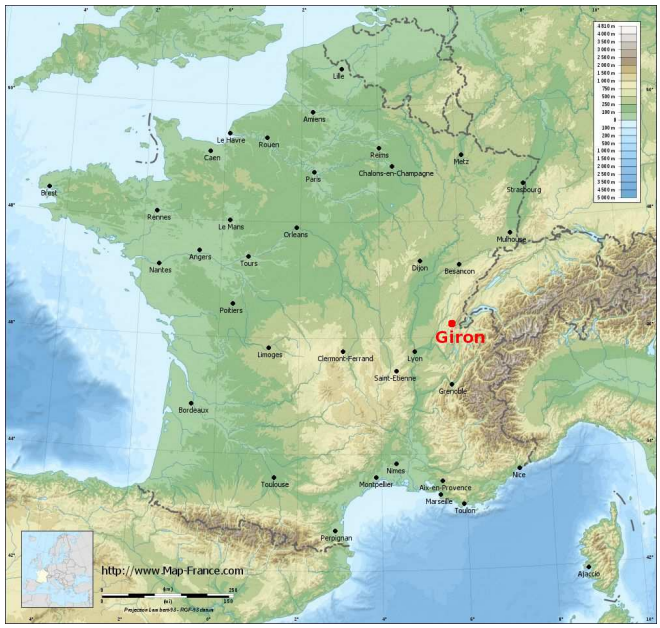

Figure 1 – Location of the IMC 2014 site on the map of France.

IMO bibcode WGN-416-roggemans-imc2014 NASA-ADS bibcode 2013JIMO...41..177R

Solar Longitudes for 2014

Compiled by Rainer Arlt

A conversion table of dates to solar longitudes using (Steyaert, 1991) is given as every year. The longitudes are given on the next page; they are only valid for 2014. The conversion formulae for any time of the day are repeated here for your convenience.

If you want to calculate the solar longitude $\lambda_\odot$ of a specific time of the day, you may use a linear interpolation between two dates. Suppose you have a certain *Date* and the *Time* in hours (UT), you get the solar longitude by

$$\lambda_\odot = \lambda_{\odot,\mathrm{Date}} + (\lambda_{\odot,\mathrm{NextDay}} - \lambda_{\odot,\mathrm{Date}}) \times \frac{\mathrm{Time}}{24\ ^\mathrm{h}}.$$

Alternatively, if you want to convert a certain solar longitude $\lambda_\odot$ into a time of the day, look up the *Date* with the next-smaller solar longitude in the table and calculate

$$\mathrm{Time} = \frac{(\lambda_\odot - \lambda_{\odot,\mathrm{Date}})}{(\lambda_{\odot,\mathrm{NextDay}} - \lambda_{\odot,\mathrm{Date}})} \times 24\ ^\mathrm{h}.$$

The solar longitudes of 1988–2020 are given in two-hour increments and with three decimals at `http://www.imo.net/data/solar`.

IMO bibcode WGN-416-arlt-solarlong
NASA-ADS bibcode 2013JIMO...41..177A

References

Steyaert C. (1991). "Calculating the solar longitude 2000.0". *WGN, Journal of the IMO*, **19:2**, 31–34.

Solar longitudes 2014. Dates refer to 00^h UT.

Jan	1	280.29	Mar	1	340.12	May	1	40.36	Jul	1	98.91	Sep	1	158.30	Nov	1	218.28
Jan	2	281.31	Mar	2	341.13	May	2	41.33	Jul	2	99.86	Sep	2	159.27	Nov	2	219.28
Jan	3	282.33	Mar	3	342.13	May	3	42.30	Jul	3	100.82	Sep	3	160.23	Nov	3	220.28
Jan	4	283.34	Mar	4	343.13	May	4	43.27	Jul	4	101.77	Sep	4	161.20	Nov	4	221.28
Jan	5	284.36	Mar	5	344.13	May	5	44.24	Jul	5	102.72	Sep	5	162.17	Nov	5	222.29
Jan	6	285.38	Mar	6	345.14	May	6	45.21	Jul	6	103.68	Sep	6	163.14	Nov	6	223.29
Jan	7	286.40	Mar	7	346.14	May	7	46.17	Jul	7	104.63	Sep	7	164.11	Nov	7	224.29
Jan	8	287.42	Mar	8	347.14	May	8	47.14	Jul	8	105.58	Sep	8	165.08	Nov	8	225.29
Jan	9	288.44	Mar	9	348.14	May	9	48.11	Jul	9	106.54	Sep	9	166.05	Nov	9	226.30
Jan	10	289.46	Mar	10	349.14	May	10	49.08	Jul	10	107.49	Sep	10	167.02	Nov	10	227.30
Jan	11	290.48	Mar	11	350.14	May	11	50.04	Jul	11	108.44	Sep	11	167.99	Nov	11	228.31
Jan	12	291.50	Mar	12	351.14	May	12	51.01	Jul	12	109.40	Sep	12	168.96	Nov	12	229.31
Jan	13	292.52	Mar	13	352.13	May	13	51.97	Jul	13	110.35	Sep	13	169.94	Nov	13	230.32
Jan	14	293.53	Mar	14	353.13	May	14	52.94	Jul	14	111.30	Sep	14	170.91	Nov	14	231.32
Jan	15	294.55	Mar	15	354.13	May	15	53.90	Jul	15	112.26	Sep	15	171.88	Nov	15	232.33
Jan	16	295.57	Mar	16	355.12	May	16	54.87	Jul	16	113.21	Sep	16	172.86	Nov	16	233.34
Jan	17	296.59	Mar	17	356.12	May	17	55.83	Jul	17	114.16	Sep	17	173.83	Nov	17	234.34
Jan	18	297.61	Mar	18	357.11	May	18	56.79	Jul	18	115.12	Sep	18	174.81	Nov	18	235.35
Jan	19	298.62	Mar	19	358.11	May	19	57.76	Jul	19	116.07	Sep	19	175.79	Nov	19	236.36
Jan	20	299.64	Mar	20	359.10	May	20	58.72	Jul	20	117.03	Sep	20	176.76	Nov	20	237.37
Jan	21	300.66	Mar	21	0.10	May	21	59.68	Jul	21	117.98	Sep	21	177.74	Nov	21	238.38
Jan	22	301.68	Mar	22	1.09	May	22	60.64	Jul	22	118.94	Sep	22	178.72	Nov	22	239.39
Jan	23	302.69	Mar	23	2.08	May	23	61.61	Jul	23	119.89	Sep	23	179.70	Nov	23	240.40
Jan	24	303.71	Mar	24	3.07	May	24	62.57	Jul	24	120.85	Sep	24	180.68	Nov	24	241.41
Jan	25	304.73	Mar	25	4.06	May	25	63.53	Jul	25	121.80	Sep	25	181.65	Nov	25	242.42
Jan	26	305.75	Mar	26	5.06	May	26	64.49	Jul	26	122.76	Sep	26	182.63	Nov	26	243.43
Jan	27	306.76	Mar	27	6.05	May	27	65.45	Jul	27	123.71	Sep	27	183.62	Nov	27	244.45
Jan	28	307.78	Mar	28	7.04	May	28	66.41	Jul	28	124.67	Sep	28	184.60	Nov	28	245.46
Jan	29	308.80	Mar	29	8.03	May	29	67.37	Jul	29	125.62	Sep	29	185.58	Nov	29	246.47
Jan	30	309.81	Mar	30	9.01	May	30	68.33	Jul	30	126.58	Sep	30	186.56	Nov	30	247.48
Jan	31	310.83	Mar	31	10.00	May	31	69.29	Jul	31	127.54						
Feb	1	311.84	Apr	1	10.99	Jun	1	70.25	Aug	1	128.49	Oct	1	187.54	Dec	1	248.50
Feb	2	312.86	Apr	2	11.98	Jun	2	71.21	Aug	2	129.45	Oct	2	188.53	Dec	2	249.51
Feb	3	313.87	Apr	3	12.96	Jun	3	72.17	Aug	3	130.41	Oct	3	189.51	Dec	3	250.52
Feb	4	314.89	Apr	4	13.95	Jun	4	73.12	Aug	4	131.37	Oct	4	190.49	Dec	4	251.54
Feb	5	315.90	Apr	5	14.94	Jun	5	74.08	Aug	5	132.32	Oct	5	191.48	Dec	5	252.55
Feb	6	316.92	Apr	6	15.92	Jun	6	75.04	Aug	6	133.28	Oct	6	192.46	Dec	6	253.57
Feb	7	317.93	Apr	7	16.90	Jun	7	76.00	Aug	7	134.24	Oct	7	193.45	Dec	7	254.58
Feb	8	318.94	Apr	8	17.89	Jun	8	76.95	Aug	8	135.20	Oct	8	194.44	Dec	8	255.60
Feb	9	319.95	Apr	9	18.87	Jun	9	77.91	Aug	9	136.15	Oct	9	195.42	Dec	9	256.61
Feb	10	320.97	Apr	10	19.85	Jun	10	78.86	Aug	10	137.11	Oct	10	196.41	Dec	10	257.63
Feb	11	321.98	Apr	11	20.83	Jun	11	79.82	Aug	11	138.07	Oct	11	197.40	Dec	11	258.64
Feb	12	322.99	Apr	12	21.82	Jun	12	80.78	Aug	12	139.03	Oct	12	198.39	Dec	12	259.66
Feb	13	324.00	Apr	13	22.80	Jun	13	81.73	Aug	13	139.99	Oct	13	199.38	Dec	13	260.67
Feb	14	325.01	Apr	14	23.78	Jun	14	82.69	Aug	14	140.95	Oct	14	200.36	Dec	14	261.69
Feb	15	326.02	Apr	15	24.76	Jun	15	83.64	Aug	15	141.91	Oct	15	201.36	Dec	15	262.71
Feb	16	327.03	Apr	16	25.73	Jun	16	84.60	Aug	16	142.87	Oct	16	202.35	Dec	16	263.73
Feb	17	328.04	Apr	17	26.71	Jun	17	85.55	Aug	17	143.83	Oct	17	203.34	Dec	17	264.74
Feb	18	329.05	Apr	18	27.69	Jun	18	86.51	Aug	18	144.79	Oct	18	204.33	Dec	18	265.76
Feb	19	330.06	Apr	19	28.67	Jun	19	87.46	Aug	19	145.75	Oct	19	205.32	Dec	19	266.78
Feb	20	331.07	Apr	20	29.64	Jun	20	88.41	Aug	20	146.72	Oct	20	206.32	Dec	20	267.80
Feb	21	332.07	Apr	21	30.62	Jun	21	89.37	Aug	21	147.68	Oct	21	207.31	Dec	21	268.82
Feb	22	333.08	Apr	22	31.60	Jun	22	90.32	Aug	22	148.64	Oct	22	208.31	Dec	22	269.83
Feb	23	334.09	Apr	23	32.57	Jun	23	91.28	Aug	23	149.61	Oct	23	209.30	Dec	23	270.85
Feb	24	335.09	Apr	24	33.55	Jun	24	92.23	Aug	24	150.57	Oct	24	210.30	Dec	24	271.87
Feb	25	336.10	Apr	25	34.52	Jun	25	93.19	Aug	25	151.54	Oct	25	211.29	Dec	25	272.89
Feb	26	337.11	Apr	26	35.49	Jun	26	94.14	Aug	26	152.50	Oct	26	212.29	Dec	26	273.91
Feb	27	338.11	Apr	27	36.47	Jun	27	95.09	Aug	27	153.47	Oct	27	213.29	Dec	27	274.93
Feb	28	339.12	Apr	28	37.44	Jun	28	96.05	Aug	28	154.43	Oct	28	214.29	Dec	28	275.95
			Apr	29	38.41	Jun	29	97.00	Aug	29	155.40	Oct	29	215.28	Dec	29	276.97
			Apr	30	39.39	Jun	30	97.96	Aug	30	156.36	Oct	30	216.28	Dec	30	277.99
									Aug	31	157.33	Oct	31	217.28	Dec	31	279.01

Meteor science

General relativistic precession in meteoroid orbits

A. Sekhar [1, 2]

There are only very few past works related to the application of general relativity in the orbital evolution of small solar system bodies. Previous calculations have shown that mean motion resonances due to Jupiter and Saturn can enable meteoroids to stay resonant for the order of few thousand years. Now we study the general relativistic precession for such long term evolution of meteoroid particles and its subsequent effects in nodal displacements. Our calculations show that although the Newtonian model works very well for almost all practical purposes for the well known showers during present epochs, there could be some exceptional combinations of orbital elements for which the general relativistic precession in argument of pericentre and its influence on nodal distances could become significantly pronounced and decisive for predicting any earth-meteor intersection. In this work we present some calculations proving these aspects in the context of well known and active meteor showers namely Geminids, Orionids and Leonids. A similar analysis is done on low perihelion distance and low semi-major axis meteoroid streams taken from the list of established showers at the IAU-Meteor Data Center.

Submitted on 2013 May 17

1 Introduction

One of the greatest triumphs of general relativity (GR) was the prediction (Einstein 1915) and subsequent confirmation of the precession of perihelion of Mercury. Ever since this important discovery, only very few works (Fox et al., 1982; Sitarski, 1992; Shahid-Saless & Yeomans, 1994; Venturini & Gallardo, 2010) have undertaken applications of general relativity in the long term orbital evolution of small solar system bodies.

Previous calculations (Rendtel, 2007; Sato & Watanabe, 2007; Sekhar & Asher, 2013a; Sekhar & Asher, 2013b) have shown that the resonant structures (due to both Jupiter & Saturn) in meteoroid streams can retain their compact structures for the order of few thousand years. During that time frame, changes in a & e are quite small for the purpose of study presented here. There are various previous works (Yeomans, 1981; Asher & Clube, 1993; Jenniskens et al., 1998; Asher et al., 1999; McNaught & Asher, 1999; Brown, 2001; Ryabova, 2003; Lyytinen & van Flandern, 2004; Rudawska et al., 2005; Watanabe et al., 2005; Wiegert & Brown, 2005; Vaubaillon et al., 2006; Jenniskens et al., 2007; Maslov, 2007; Rendtel, 2007; Sato & Watanabe, 2007; Christou et al., 2008; Soja et al., 2011; Sekhar & Asher, 2013a; Sekhar & Asher, 2013b) which focus on dust trails evolving for hundreds to many thousands of years. It would be worthwhile to look at the effects of general relativistic precession for such long term evolution of meteoroid orbits and check whether such effects are important in the long term prediction of meteor outbursts or storms.

Relativistic effects would get more pronounced when a body moves with high velocities. Hence low perihelion distance (q) would lead (due to Kepler's second law) to greater precession per revolution. Since this precession occurs during every perihelion passage, a larger number of revolutions means this effect accumulates very efficiently over a long period of time. In short, a body with small q and small a will have maximum contribution due to relativistic precession. Another important effect when a body comes very close to a massive rotating body is the Lense-Thirring effect which is manifested due to the dragging of space-time by a rotating body (Iorio, 2005). It is not included in our calculations in this work mainly because it is typically four orders of magnitude smaller (Iorio, 2005) than the effect discussed here.

2 Drift in argument of pericentre due to GR and its subsequent effect on nodal distances

Change in the argument of pericentre (ω) of an orbit is given by (page 197, Weinberg 1972):

$$\Delta\omega = \frac{6\pi GM}{a(1-e^2)} \tag{1}$$

where a and e are the semi-major axis and eccentricity of the orbit respectively. Equation (1) gives the result in radians/revolution. The same expression can be applied to any cometary/meteoroid orbit in the solar system (Fox et al., 1982; Shahid-Saless & Yeomans, 1994).

$$r_a = \frac{a(1-e^2)}{(1+e\ cos\omega)} \tag{2}$$

$$r_d = \frac{a(1-e^2)}{(1-e\ cos\omega)} \tag{3}$$

Equation (2) gives the expression for the heliocentric distance of ascending node (r_a) for Orionids. Equation (3) gives the expression for the heliocentric distance of descending node (r_d) for Leonids and Geminids. These

[1]Armagh Observatory, College Hill, Armagh BT61 9DG, United Kingdom
[2]Queen's University of Belfast, University Road, Belfast BT7 1NN, United Kingdom
Email: asw@arm.ac.uk , asekhar01@qub.ac.uk

IMO bibcode WGN-416-sekhar-gr
NASA-ADS bibcode 2013JIMO...41..179S

Table 1 – $\Delta\omega$ and Δr due to general relativistic effects for different parent bodies and meteoroid streams in 1000 years.

Body/Meteoroid Stream	q (AU)	a (AU)	e	ω (Degrees)	$\Delta\omega$ ($\times 10^{-2}$ Degrees)	Δr ($\times 10^{-4}$AU)
Icarus	0.187	1.078	0.827	31.348	2.8	8.3
Phaethon	0.140	1.271	0.890	322.148	2.7	8.0
Geminids	0.141	1.372	0.890	324.420	2.3	7.7
Halley	0.575	17.871	0.968	112.279	0.013	0.054
Orionids	0.578	18.000	0.968	81.500	0.012	0.018
Tempel-Tuttle	0.977	10.337	0.906	172.499	0.017	0.0020
Leonids	0.984	10.300	0.904	172.400	0.017	0.0019

Table 2 – $\Delta\omega$ and Δr for different low q ($\leq$ 0.15 AU) and low a ($\leq$ 1.5 AU) meteoroid streams (taken from the list of established meteor showers in IAU-MDC) due to general relativistic precession in 1000 years.

IAU Code	Meteoroid Stream	q (AU)	a (AU)	ω (Degrees)	$\Delta\omega$ ($\times 10^{-2}$ Degrees)	Δr ($\times 10^{-3}$AU)
004 GEM	Geminids	0.141	1.372	324.420	2.3	0.77
164 NZC	Northern June Aquilids	0.114	1.348	329.500	3.1	1.3
390 THA	November θ Aurigids	0.116	1.130	330.070	4.0	1.4
165 SZC	Southern June Aquilids	0.110	1.150	152.000	4.1	1.6
152 NOC	North. Daytime ω Cetids	0.108	0.967	25.600	5.4	1.9
171 ARI	Daytime Arietids	0.085	1.376	25.900	4.0	2.0

two quantities are critical for any meteor shower prediction calculations because the heliocentric distances of ascending or descending node should be close to Earth's orbit in order to produce any meteor activity. Hence significant changes in these parameters can directly decide the outcome of shower prediction models.

The relationship between the change in nodal distances (Δr) with respect to the change in argument of pericentre ($d\omega$) could be computed by differentiating equation (2) and (3).

$$dr_a = \frac{ae(1-e^2)\ sin\omega\ d\omega}{(1+e\ cos\omega)^2} \tag{4}$$

$$dr_d = \frac{-ae(1-e^2)\ sin\omega\ d\omega}{(1-e\ cos\omega)^2} \tag{5}$$

The values of $\Delta\omega$ and Δr given in Table 1 and 2 are calculated using the equations (1), (4) and (5). The orbital elements a,e and ω of 1P/Halley (JD 2456400.5), 55P/Tempel-Tuttle (JD 2450880.5), 3200 Phaethon (JD 2456400.5) and 1566 Icarus (JD 2456400.5) are taken for epochs (mentioned in brackets) from IAU-Minor Planet Center. Orbital parameters for various meteoroid streams are substituted from IAU-Meteor Data Center. It can be clearly seen that $\Delta\omega$ in Geminids is about 100 times that of Leonids and Orionids for an orbital evolution of 1000 years. Subsequently our calculations show that Δr due to $\Delta\omega$ in Geminids can be around 1000 times of that in Leonids. Overall the substantial effect of GR in low q showers compared to other showers can be understood from this analysis. Calculations for Icarus were done because it is a well known low q body and has the highest precession rate due to GR among small solar system bodies. Hence it is a good example to compare with other parent bodies. Although the orbital elements of meteoroid streams are slightly different from those of the corresponding parent bodies, the changes in $\Delta\omega$ and Δr are practically small in terms of order of magnitude (as shown in Table 1).

Table 2 shows the list of established meteor showers which have low q ($\leq$ 0.15 AU) and low a ($\leq$ 1.5 AU). All the orbital elements are taken from IAU-Meteor Data Center. Although the parent bodies of most showers in this list are not confirmed, it is still worthwhile to calculate and compare the GR precession and the subsequent nodal displacement in these streams. We find that the Northern Daytime ω Cetids have the highest rate of GR precession in ω ($\Delta\omega \sim 5.4 \times 10^{-2}$ degrees in 1 kyr). Low values of q and a make this stream apt for efficient accumulation of the GR effect over many revolutions. However the maximum Δr ($\sim 2 \times 10^{-3}$ AU in 1 kyr) is exhibited by Daytime Arietids due to low q and low a compounded by the favourable value in ω.

3 Values of argument of pericentre for maximum change in nodal distances

Equations (4) and (5) show that Δr at any instant would depend on ω for a constant value of $\Delta\omega$.

Numerical solutions were done (see Figures 1,2 and 3) to compute the limiting values of ω. Figures 1 and 3 show that Δr in Geminids and Leonids has extreme values when $\omega \sim 16°$ and 343°. Figure 2 indicates that Δr in Orionids has peak values when $\omega \sim 171°$ and 188°. Understanding the maximum change in nodal distances is crucial in meteor forecast models.

Please note Y-axis scale for Figure 1 representing Geminids. It clearly shows how substantial the error (of the order of 10^{-3} AU) in nodal distances (if GR effects are not included) could be, when the particles have $\omega \sim$

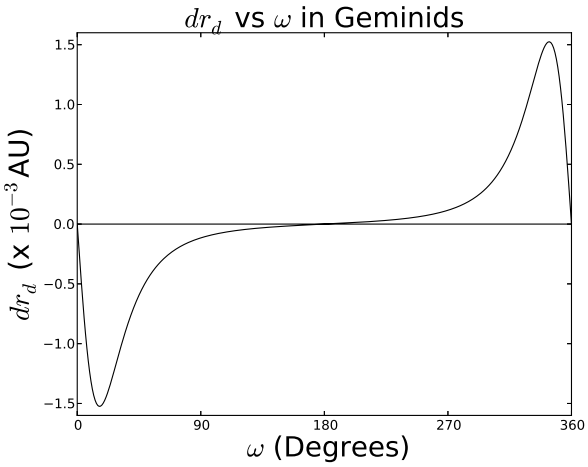

Figure 1 – Change in heliocentric distance of descending node in Geminids for different values of argument of pericentre for a constant $\Delta\omega$=2.3 × 10^{-2} degrees/kyr

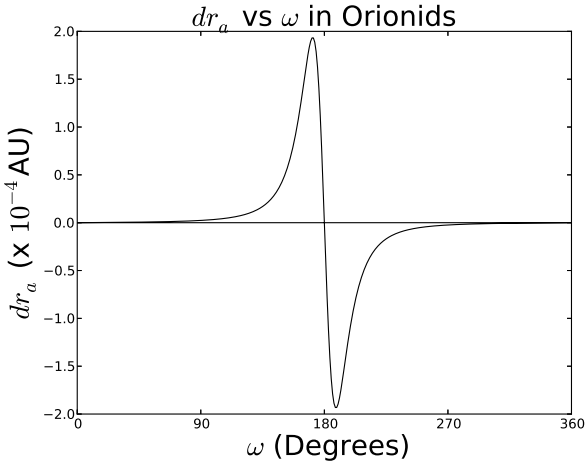

Figure 2 – Change in heliocentric distance of ascending node in Orionids for various values of argument of pericentre for a constant $\Delta\omega$=1.2 × 10^{-4} degrees/kyr

343° during its past or future. In such cases, general relativistic precession could actually play as decisive a factor in the intersection or miss of a concentrated dust trail with Earth (diameter ∼ 10^{-4} AU) when long term predictions (of the order of kyr) are involved. During present times, Geminids have $\omega \sim 324°$ (IAU-Meteor Data Center) which is not too far from producing an error of the order of 10^{-3} AU when GR effects are ignored. All other established meteoroid streams in Table 2 have $\Delta r \sim 10^{-3}$ AU. Previous calculations (Asher et al., 1999; McNaught & Asher, 1999) have shown that the Leonid meteor storms in the past were caused by dust trails with widths of the order of 10^{-3} AU.

One could find these limiting values in ω analytically as well, for clarity and rigour. The simple analytical approach (using standard techniques in calculus) is described below.

$$\frac{d^2r_a}{d\omega^2} = \frac{ae(1-e^2)[(1+e\ cos\omega)\ cos\omega + 2e\ sin^2\omega]}{(1+e\ cos\omega)^3} \quad (6)$$

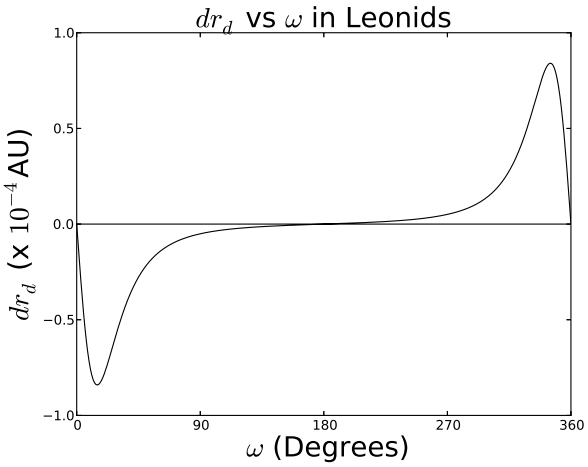

Figure 3 – Change in heliocentric distance of descending node in Leonids for all possible values of argument of pericentre for a constant $\Delta\omega$=1.7 × 10^{-4} degrees/kyr

$$\frac{d^2r_d}{d\omega^2} = \frac{-ae(1-e^2)[(1-e\ cos\omega)\ cos\omega - 2e\ sin^2\omega]}{(1-e\ cos\omega)^3} \quad (7)$$

Equations (6) and (7) gives the derivative of equations (4) and (5) respectively. In order to find the value of ω corresponding to the extreme values of Δr_a and Δr_d, equations (6) and (7) can be equated to zero.

$$\frac{d^2r_a}{d\omega^2} = 0 \quad (8)$$

$$\frac{d^2r_d}{d\omega^2} = 0 \quad (9)$$

Substituting the expressions in equation (6) and (7) into equations (8) and (9) respectively and further simplification of above expressions yield:

$$e\ cos^2\omega - cos\omega - 2e = 0 \quad (10)$$

$$e\ cos^2\omega + cos\omega - 2e = 0 \quad (11)$$

Solving the simple quadratic equations (10) and (11) give two roots each, of which only one corresponds to the real case:

$$\omega = cos^{-1}[(1 - \sqrt{(1+8e^2)})/2e] \quad (12)$$

Equation (12) shows the real root which corresponds to specific values of ω leading to maximum dr_a. The extreme values for dr_a in Orionids occur when $\omega \sim 171°$ and 188°.

$$\omega = cos^{-1}[(-1 + \sqrt{(1+8e^2)})/2e] \quad (13)$$

Equation (13) gives the real root for specific cases of ω which can produce extreme values of dr_d. The maximum values for dr_d in Leonids and Geminids appear when $\omega \sim 16°$ and 343°. The analytical treatment perfectly matches with the numerical solutions shown in Figures 1, 2 and 3. Hence it is a parallel verification of the whole analysis.

4 Conclusion

In this work we find that, for the well known showers during present epochs, the drifts in ω and subsequent changes in nodal distances are quite small compared to other errors and effects in meteor shower predictions on a time scale of 1000 yr. Hence a simple Newtonian model for the precise prediction of meteor-earth intersections does apply successfully for most of the cases.

However it is important to note that precession due to GR is independent of the size of the particle unlike radiation pressure, Poynting-Robertson effect, Yarkovsky effect etc. Furthermore it would accumulate over time and would not get nullified or corrected directly by other effects.

It is evident that evolution of small meteoroid particles (with diameters ≤ 1 mm) would be dominated by various radiative forces. This would in turn mean that only the large particles accumulate the GR precession effectively over such long time scales.

For example in the well known case of Geminids, Δr is about 1000 times that of present day Leonids because of larger $\Delta\omega$ from relativistic precession and initial ω favouring the near maxima of Δr. It is found that the low q shower Northern Daytime ω Cetids has the highest rate of GR precession in ω ($\Delta\omega \sim 5.4 \times 10^{-2}$ degrees in 1 kyr) out of all the established meteoroid streams so far. The maximum Δr ($\sim 2 \times 10^{-3}$ AU in 1 kyr) is seen in Daytime Arietids due to its low q and low a coupled with the favourable value in ω. Changes in r in this range can be crucial for meteor outburst/storm forecast models. This proves that there could be interesting exceptions (regarding accuracy of Newtonian model) for some particular combinations of q, e & ω of the meteoroid streams where GR effects have to be taken into account for accurate meteor shower forecasts.

Acknowledgments

Author thanks the anonymous reviewer for the helpful comments. I am grateful to my research supervisor Dr D J Asher for all his suggestions to improve the manuscript. Research at Armagh Observatory is funded by the Department of Culture, Arts and Leisure of Northern Ireland.

References

Asher D. J., Bailey M. E., and Emel'Yanenko V. V. (1999). "Resonant meteoroids from Comet Tempel-Tuttle in 1333: the cause of the unexpected Leonid outburst in 1998". *MNRAS*, **304**, L53–L56.

Asher D. J. and Clube S. V. M. (1993). "An Extraterrestrial Influence during the Current Glacial-Interglacial". *QJRAS*, **34**, 481–511.

Brown P. G. (2001). *Evolution of Two periodic Meteoroid Streams: the Perseids and Leonids*. PhD thesis, University of Western Ontario.

Christou A. A., Vaubaillon J., and Withers P. (2008). "The P/Halley Stream: Meteor Showers on Earth, Venus and Mars". *Earth Moon and Planets*, **102**, 125–131.

Fox K., Williams I. P., and Hughes D. W. (1982). "The evolution of the orbit of the Geminid meteor stream". *MNRAS*, **200**, 313–324.

Iorio L. (2005). "Is it possible to measure the Lense-Thirring effect on the orbits of the planets in the gravitational field of the Sun?". *A&A*, **431**, 385–389.

Jenniskens P., Betlem H., de Lignie M., Ter Kuile C., van Vliet M. C. A., van 't Leven J., Koop M., Morales E., and Rice T. (1998). "On the unusual activity of the Perseid meteor shower (1989-96) and the dust trail of comet 109P/Swift-Tuttle". *MNRAS*, **301**, 941–954.

Jenniskens P., Lyytinen E., Nissinen M., Yrjola I., and Vaubaillon J. (2007). "Strong Ursid shower predicted for 2007 December 22". *WGN, Journal of the IMO*, **35**, 125–133.

Lyytinen E. and van Flandern T. (2004). "Perseid one-revolution outburst in 2004". *WGN, Journal of the IMO*, **32**, 51–53.

Maslov M. (2007). "Leonid predictions for the period 2001-2100". *WGN, Journal of the IMO*, **35**, 5–12.

McNaught R. H. and Asher D. J. (1999). "Leonid Dust Trails and Meteor Storms". *WGN, Journal of the IMO*, **27**, 85–102.

Rendtel J. (2007). "Three days of enhanced Orionid activity in 2006 - Meteoroids from a resonance region?". *WGN, Journal of the IMO*, **35**, 41–45.

Rudawska R., Jopek T. J., and Dybczyński P. A. (2005). "The Changes of the Orbital Elements and Estimation of the Initial Velocities of Stream Meteoroids Ejected from Comets and Asteroids". *Earth Moon and Planets*, **97**, 295–310.

Ryabova G. O. (2003). "The comet Halley meteoroid stream: just one more model". *MNRAS*, **341**, 739–746.

Sato M. and Watanabe J.-I. (2007). "Origin of the 2006 Orionid Outburst". *PASJ*, **59**, L21.

Sekhar A. and Asher D. J. (2013a). "Resonant behavior of comet Halley and the Orionid stream". *Meteoritics and Planetary Science*.

Sekhar A. and Asher D. J. (2013b). "Saturnian mean motion resonances in meteoroid streams". *MNRAS*, **433**, L84–L88.

Shahid-Saless B. and Yeomans D. K. (1994). "Relativistic effects on the motion of asteroids and comets". *AJ*, **107**, 1885–1889.

Sitarski G. (1992). "On the relativistic motion of (1566) Icarus". *AJ*, **104**, 1226–1229.

Soja R. H., Baggaley W. J., Brown P., and Hamilton D. P. (2011). "Dynamical resonant structures in meteoroid stream orbits". *MNRAS*, **414**, 1059–1076.

Vaubaillon J., Lamy P., and Jorda L. (2006). "On the mechanisms leading to orphan meteoroid streams". *MNRAS*, **370**, 1841–1848.

Venturini J. and Gallardo T. (2010). "How to take into account the relativistic effects in dynamical studies of comets". In Fernandez J. A., Lazzaro D., Prialnik D., and Schulz R., editors, *IAU Symposium*, volume 263. pages 106–109.

Watanabe J.-I., Sato M., and Kasuga T. (2005). "Phoenicids in 1956 Revisited". *PASJ*, **57**, L45–L49.

Weinberg S. (1972). *Gravitation and Cosmology: Principles and Applications of the General Theory of Relativity*. Wiley-VCH, 688 pages.

Wiegert P. and Brown P. (2005). "The Quadrantid meteoroid complex". *Icarus*, **179**, 139–157.

Yeomans D. K. (1981). "Comet Tempel-Tuttle and the Leonid meteors". *Icarus*, **47**, 492–499.

Handling Editor: Javor Kac
This paper has been typeset from a LaTeX file prepared by the author.

Letter — The CMN catalogue of orbits for 2011

Croatian Meteor Network [1]

The Croatian Meteor Network (CMN) has released its catalogue of orbits for 2011. The catalogue contains 7770 orbits. It can be accessed from the CMN download page:
`http://cmn.rgn.hr/downloads/downloads.html`

IMO bibcode WGN-416-cmn-letter
NASA-ADS bibcode 2013JIMO...41..183C

Results of the CAMS project in 2012

Carl Johannink [1]

In early 2012 four Stations equipped with CAMS started a network in the Netherlands. In this article we present the results of the first year of the new CAMS network. Weather was rather uncooperative during most major streams but in spite of this impressive results were obtained. Two new stations were included in the network during 2012.

Received 2013 May 17

1 Introduction

After the successful Orionid project (Johannink, 2013) plans were made to set up a number of stations in the Netherlands to use this software to collect data about meteors. Thanks to the enthusiastic cooperation of Martin Breukers and Klaas Jobse, the plans materialized in the beginning of 2012. Klaas found Piet Neels at Ooltgensplaat (Netherlands) as a sparring partner at a suitable distance for double station work. Martin Breukers and the author made another duo. The locations are indicated in Figure 1. When all the technical problems were solved, Klaas, Piet and Martin were operational in March 2012 and the author got started in April 2012. The first simultaneous meteors were recorded by Klaas and Piet in March 2012 and the results were most promising. The first major meteor stream, the April Lyrids, was missed due to unfortunate weather circumstances. Better results were recorded in May. The recorded double station meteors are compared to the radiant positions and orbital elements listed in the IAU meteor stream catalogue and the Catalogue of Cometary Orbits (Marsden & Williams, 2005), but March and May got only sporadic meteors recorded.

Figure 1 – Locations of the first 4 CAMS station begin 2012.

2 Procedure

All four stations started with the basic software. After calibrating the time, the software determines the starting time and the duration of each recording (the so called Capture). The next morning the tool "Reprocess" has to run to search all recorded files for meteors. It is obvious that the Desktop PC or laptop shouldn't be too slow. The author experienced that the reprocessing of the data required a lot of time on the laptop used for registration. The 6 hours of capturing required at least 6 hours of reprocessing.

The problem was solved by taking a copy of the Captured files from the registration laptop to a much faster PC at home. After the Reprocess routine all data about possible detected meteors are listed in the FTPdetectinfo-file. During the first months it became obvious that the software could be improved and a number of specialists managed to combine the recording and reprocessing routines into a 'CaptureAndDetect' module. This way you find all the data in the morning ready for analyzing. The 'CaptureAndDetect' module requires a sufficient fast processor but it is an investment that is very rewarding in time efficiency.

The next step concerns the Astrometry. In Figure 2 the screen shows the recorded frame of a particular night at left and the corresponding part from the sky according to the star catalogue after that a few data such as the center of the field of view etc. are correctly provided. It might be a bit confusing that the declination and right ascension must be provided in decimal degrees. Any mistakes may result in a different star field from the atlas at right compared to the recorded field at left.

The astrometry is very simple. Click on a star of your recorded image and click on the corresponding star in the map of the sky at right on the screen. Repeat this about 50 times. After about 10 stars the program will suggest which star in the map could match your star in the image. After identifying about 50 stars in this way you can add another 150 stars in an almost automatic way by a simple click. Then you determine the measuring accuracy and in case this accuracy isn't satisfactory you can remove stars until the accuracy is $< 1''$, maintaining at least about 100 stars. Practice proves that accurate work with the first 10 stars rewards at the end

[1]Schiefestr. 36, 48599 Gronau, Germany.
Email: c.johannink@t-online.de

IMO bibcode WGN-416-johannink-cams2012
NASA-ADS bibcode 2013JIMO...41..184J

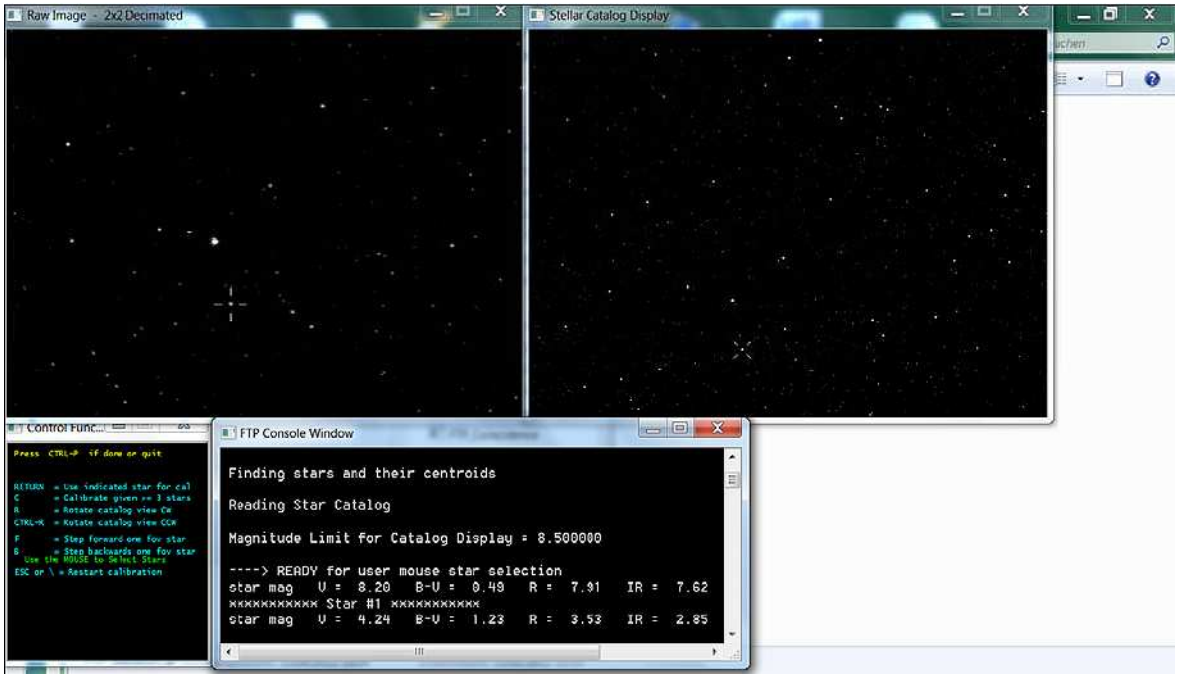

Figure 2 – The Astrometry screen: at left the recorded part of the sky and at right the related part from the star catalogue.

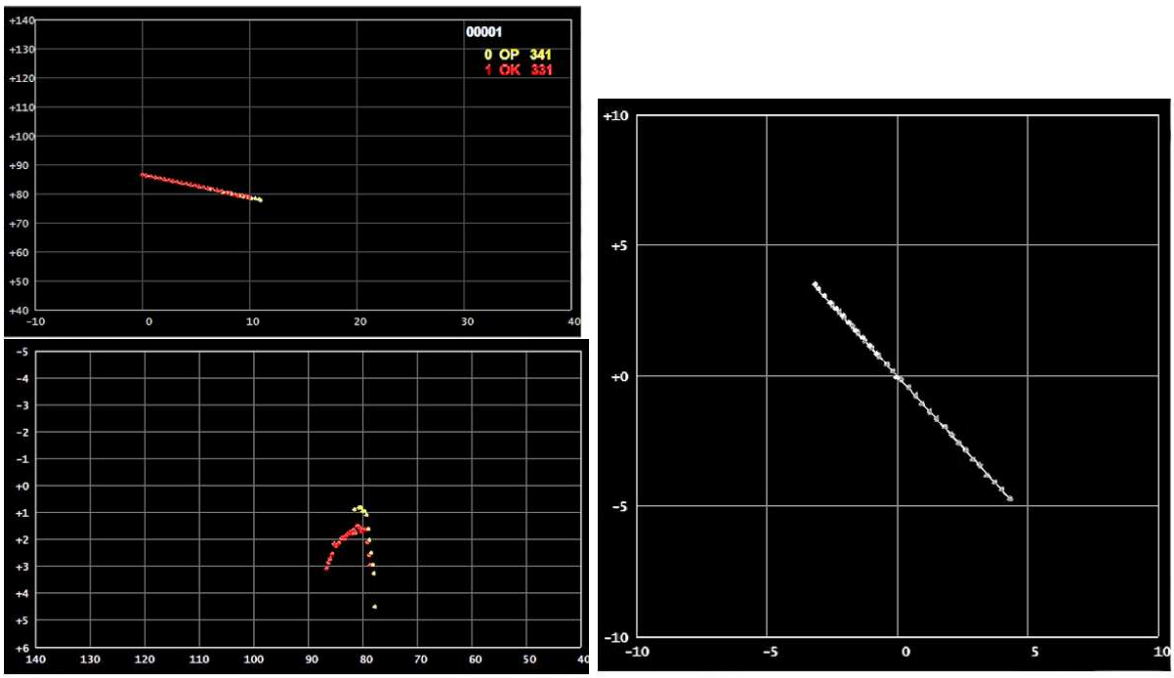

Figure 3 – the three graphical presentations in case of a candidate double station meteor. First the height against range (upper left), second latitude against longitude (right) and third magnitude against height (bottom left).

with a better accuracy. After a few trials the astrometry for the entire night is completed in about a quarter of an hour. The result is a so-called CAL-file which has to be sent to the central coordinator together with the FTPdetectinfo-file and the CameraTimeOffset file where the time difference between both double stations is described.

The tool "Coincidence" is used to search for possible double station meteors. For a night in early spring this proved to take about a half hour. In Figure 3 we display a graphical presentation of a possible simultaneous meteor between Oostkapelle and Ooltgensplaat. When this looks all right a simple click will do to record this meteor as double station. Besides the graphical presentation a txt file is automatically generated and saved with the radiant, trajectory and orbital data.

3 Results spring 2012

During spring 2012 the stations Oostkapelle (331) – Ooltgensplaat (341) and Hengelo (321) – Gronau (311) recorded 35 double station meteors and their orbits were computed. The radiant positions for Hengelo-Gronau show rather larger error margins. The rather short base

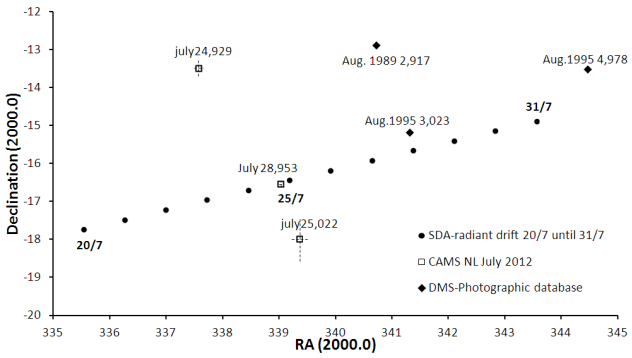

Figure 4 – SDA radiant positions for the CAMS stations compared to the radiant drift of the SDAs and SDA radiants from the DMS photographic database.

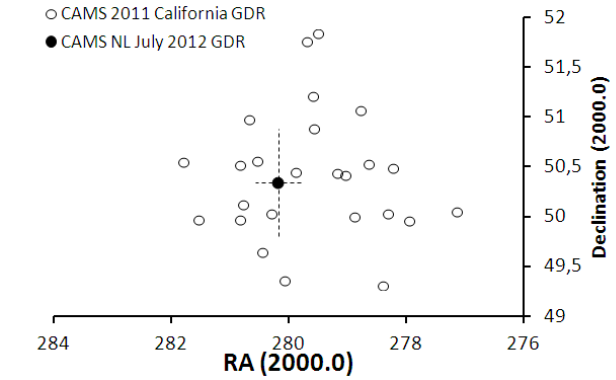

Figure 5 – Radiant positions of all simultaneously recorded CAMS from California and the simultaneously recorded Gamma Draconid from Ooltgensplaat-Oostkapelle.

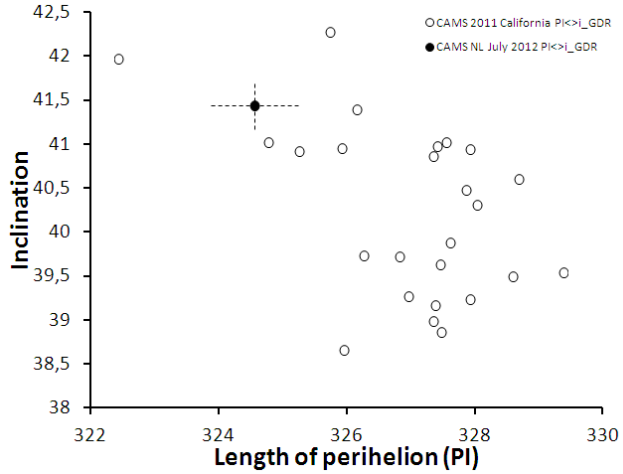

Figure 6 – Plot of the longitude of perihelion against inclination for the same dataset as Figure 5.

line between the two stations and the rather short meteor trails account for these large error margins.

4 Southern δ Aquariids July 2012

The final 10 days of July offered 6 partly clear nights and together with a single clear night begin of July this resulted in 57 double station meteors. The radiant positions for a few CAMS double stations SDAs are plotted in Figure 4, together with older radiant positions determined by DMS and the theoretical radiant drift of

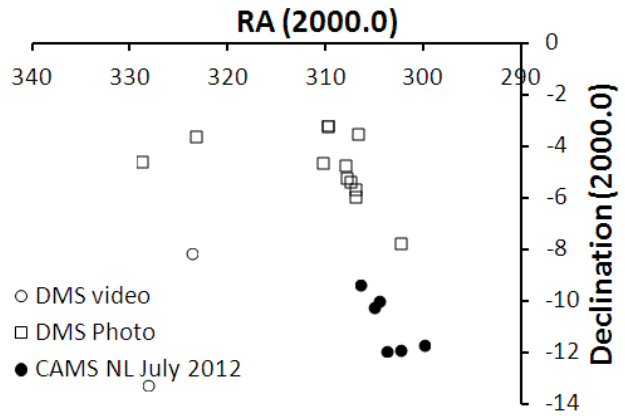

Figure 7 – radiant positions of all recently with CAMS recorded Capricornids compared with the radiant positions from the DMS photo and video database.

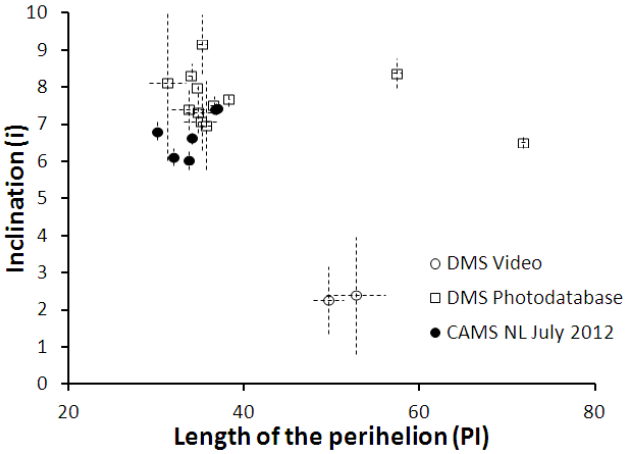

Figure 8 – Plot of the longitude of perihelion against inclination for the same dataset as Figure 7.

this stream (Jenniskens, 2006). Again the positions derived from Gronau–Hengelo show larger error bars due to the short baseline between the two stations. The radiant positions for both datasets don't fit well with the theoretical position for the date. It is possible that the Southern δ Aquariids radiant is rather diffuse but to get more conclusive results more data is required.

5 γ Draconids (GDR) July 2012

A meteor recorded on July 23 at $21^{\mathrm{h}}51^{\mathrm{m}}19^{\mathrm{s}}$ from Oostkapelle (331)–Ooltgensplaat (341) with a velocity of $V_g = 28$ km/s agrees well with the γ Draconids (Holman & Jenniskens, 2012). Figure 5 shows the radiant position together with all the γ Draconid radiants from (Holman & Jenniskens, 2012). Figure 6 plots the longitude of perihelion Π against the inclination. No doubts remain: a γ Draconid has been recorded by the new CAMS network in the Netherlands.

6 Capricornids (CAP) July 2012

It is surprising how many members of the Capricornid family were recorded compared to the SDAs. Figures 7 and 8 show respectively the radiant plot and the longitude of perihelion against inclination.

Figure 9 – Two Perseids recorded August 11 at $02^h06^m56^s$ and $02^h07^m01^s$ from Gronau (311).

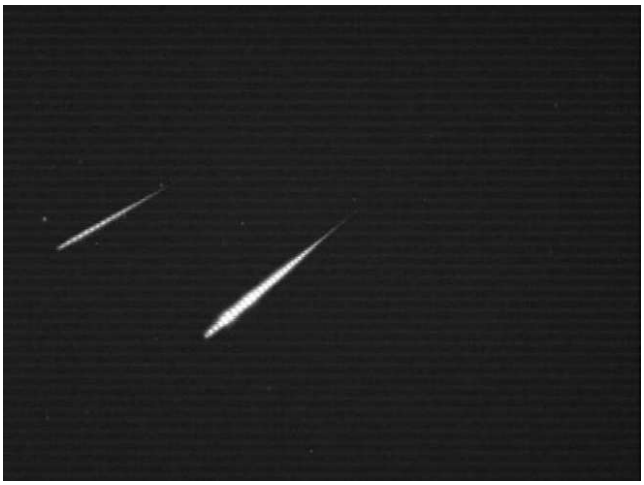

Figure 10 – Two Perseids recorded August 11 at $02^h06^m56^s$ and $02^h07^m01^s$ from Hengelo (321).

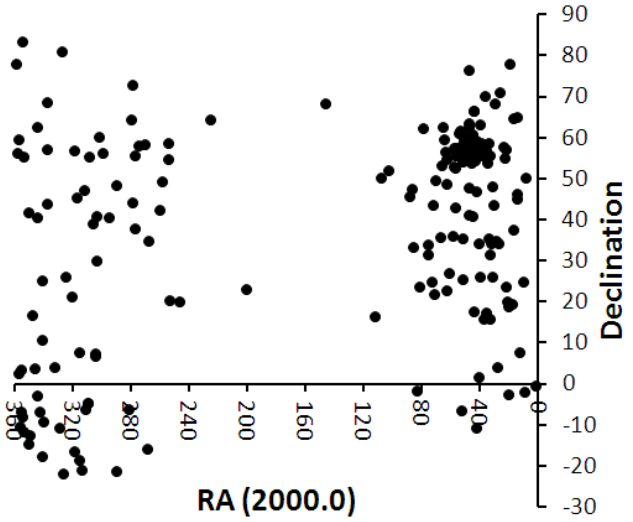

Figure 11 – Radiant positions of the 294 double station meteors in August 2012.

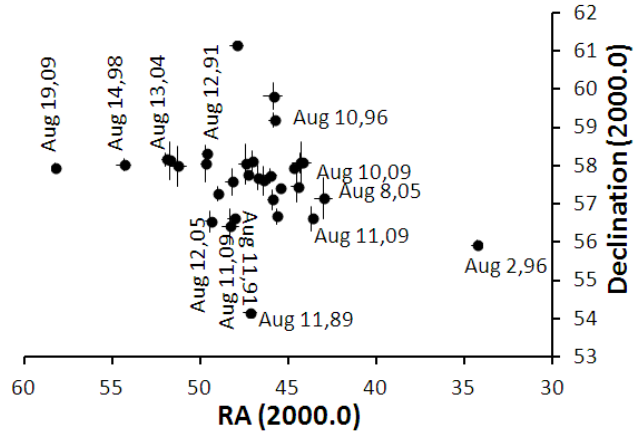

Figure 12 – The radiant distribution clearly shows the radiant drift of the Perseids.

7 August 2012

Koen Miskotte joined the network halfway August with a CAMS station at Ermelo (351). Exactly during the Perseid maximum a stable high pressure area assured clear sky during August 11–12 and 12–13 which is a rather rare phenomenon in the Netherlands. The combination Hengelo-Gronau aimed their cameras at a common area in the atmosphere in northern direction. Figure 9 and Figure 10 show two Perseids recorded by both stations at $02^h06^m56^s$ and $02^h07^m01^s$.

In total orbits for 293 double station meteors could be recorded. A plot with all the radiant positions is represented in Figure 11 which clearly shows the concentration around the Perseid radiant. Looking more in detail we can easily study the radiant drift of the Perseids from this dataset. We selected the meteors of this stream with an error margin of less than $0\overset{\circ}{.}6$ in Figure 12.

8 September 2012

During September, 173 double station meteors were recorded with the CAMS. Many nights were partly clear, but few were entirely clear. Figure 13 shows the radiant distribution.

9 Autumn 2012

The months October till December are traditionally the richest period of the year meteor wise. Unfortunately the weather was very uncooperative in the Netherlands, except for the coasts. Thanks to the stations of Klaas Jobse and Piet Neels near the coast, 495 double station meteors could be recorded. Robert Haas joined the network in October with a station at Alphen aan de Rijn (see Figure 14).

10 Orionids 2012

During the month October 220 double station meteors were recorded. Figure 15 shows the radiant positions for these meteors. Around Right Ascension $\sim 100°$ we see a cluster of radiants which are the Orionids. A bit further to the right we can notice the radiant positions for the first Taurids around $\sim 50°$ in Right Ascension.

Figure 16 focuses on the radiant positions of the Orionids and Figure 17 shows the radiant position corrected for the radiant drift. The result is a nicely concentrated cluster. Figure 18 is a plot of inclination against longitude of perihelion. The two meteors with $\pi < 90°$ were recorded on 9 and 10 October 2012 by

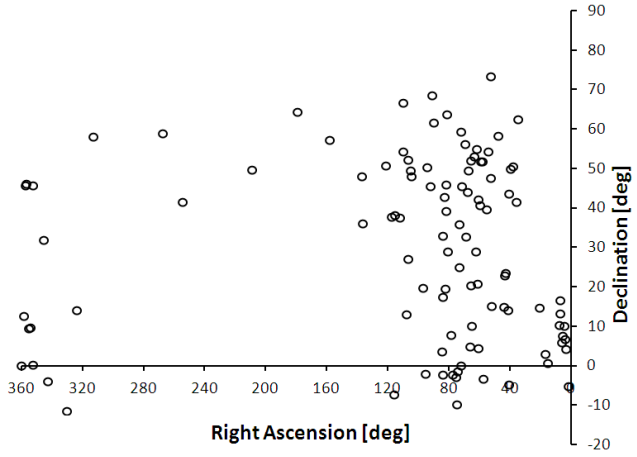

Figure 13 – Radiant positions of the 173 double station meteors in September 2012 by the CAMS stations of Oostkapelle, Ooltgensplaat, Ermelo, Hengelo and Gronau.

Figure 14 – The CAMS station at Alphen aan de Rijn.

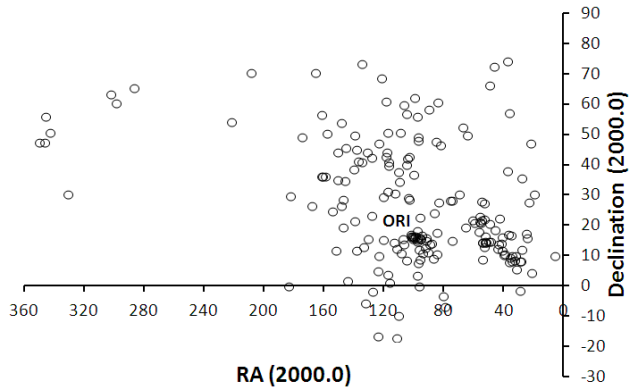

Figure 15 – The radiant positions of the 220 recorded double station meteors in October 2012 by the CAMS stations Alphen aan de Rijn, Ermelo, Gronau, Hengelo, Ooltgensplaat and Oostkapelle.

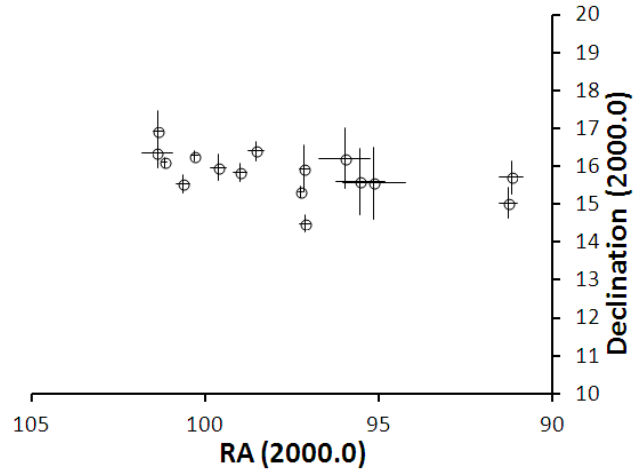

Figure 16 – Radiant positions of the double station recorded Orionids.

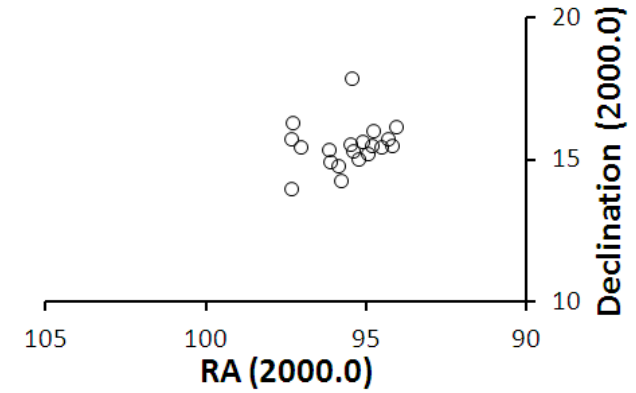

Figure 17 – Corrected radiant positions ($\lambda_\odot$ 208.0) for the Orionids.

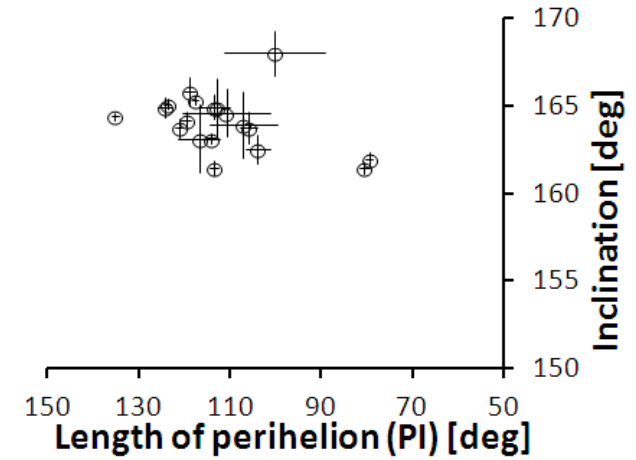

Figure 18 – Plot of the longitude of perihelion against the inclination for all meteors associated as Orionids.

Klaas Jobse and Piet Neels. The value for V_g for these meteors is $\sim$ 68 km/s and a bit higher than for the other Orionids ($V_g \sim 66$ km/s) a minor difference but meanwhile it appears these meteors were mistaken for Orionids. This indicates that meteor stream classification so long before the shower maximum remains somehow tricky. For visual observers this is a point that requires attention. One should be careful to extend the visibility periods for which the limits can be only determined by photographic and video techniques.

11 Taurids 2012

For the other cluster in the radiant plot of Figure 15, the Taurids, we made an overall picture of the radiant positions for the time span of October till December. The

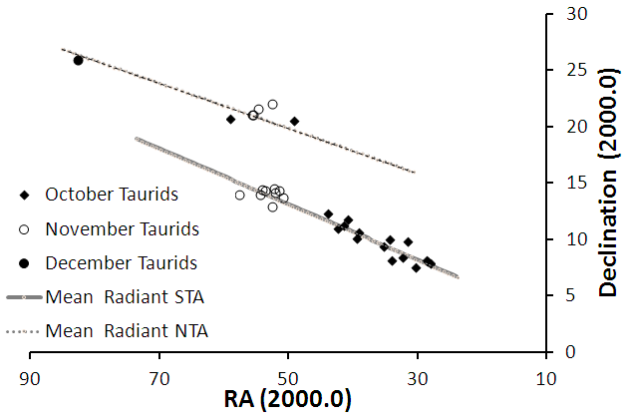

Figure 19 – Radiant positions of the double station Taurids.

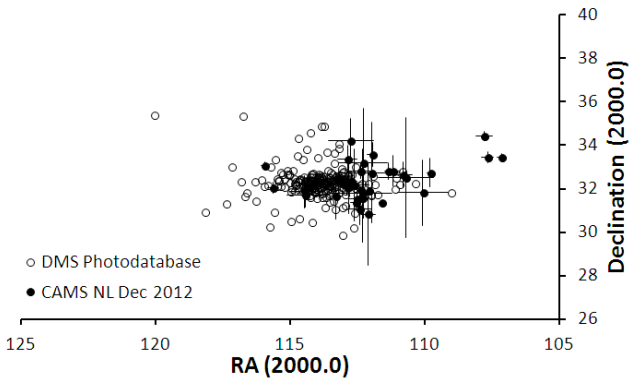

Figure 21 – The radiant positions for all double station Geminids from the DMS photographic database and CAMS.

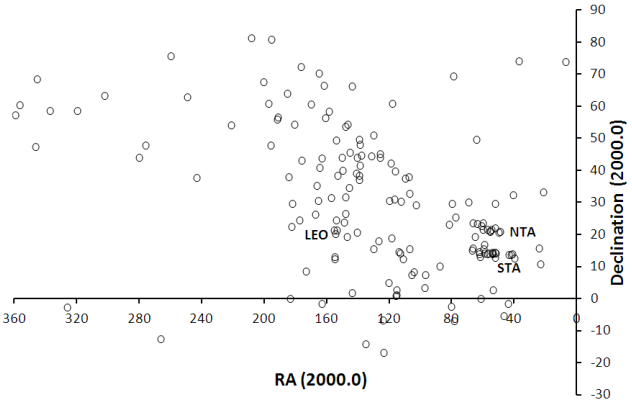

Figure 20 – Radiant positions for all 158 recorded double station meteors of November 2012 by the stations Alphen aan de Rijn, Ermelo, Gronau, Hengelo, Ooltgensplaat and Oostkapelle.

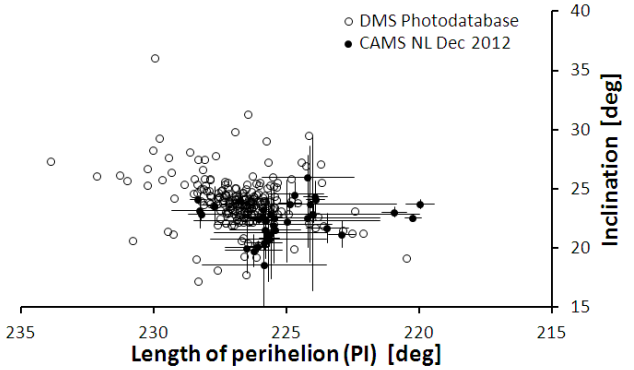

Figure 22 – Plot of the longitude of perihelion against the inclination for all Geminids from the DMS photographic database and CAMS 2012.

amount of recorded Taurids is too small in 2012 for any more detailed analyses. Figure 19 suggest again that the Taurid activity is mainly produced by the Southern branch in the first weeks of the activity (Johannink, 2013). For the results of November 2012 we present a plot of the radiant positions of the recorded double station meteors (Figure 20). Beyond the already described Taurids a small concentration occurs at Right Ascension $\sim 155°$ which indicates the presence of the Leonids.

12 December and the Geminids 2012

The successful employment of the CAMS triggered high expectations for the Geminids in December. Unfortunately the very disappointing weather circumstances hampered most observing efforts. In the night of December 12-13 Klaas Jobse and Piet Neels managed to gather some data. The analyses of this data turned out to be an exciting experience. About second by second each hit at the keyboard added a double station Geminid. In the overview plot of radiant positions for December we notice the high concentration around Right Ascension $\sim 110°$.

In Figure 21 the Geminid radiant positions are compared to the positions from the DMS photographic database. Although the positions weren't corrected for radiant drift (about 1 degree in Right Ascension per day the coincidence is really striking. This is also visible in the plot of the longitude of perihelion against the inclination for the double station Geminids from the DMS photographic database and the Geminids recorded by CAMS in December 2012 (see Figure 22).

References

Holman D. and Jenniskens P. (2012). "Confirmation of the July Gamma Draconids (GDR, IAU #184)". *WGN, Journal of the IMO*, **40:1**, 36–41.

Jenniskens P. (2006). *Meteor Showers and their parent comets*. Cambridge University Press, 691-746 pages.

Johannink C. (2013). "Results for a CAMS double-station video observation Meterik – Gronau". *WGN, Journal of the IMO*, **41:1**, 14–21.

Marsden B. G. and Williams G. V. (2005). *IAU meteor stream catalogue and the Catalogue of Cometary Orbits*. IAU Central Bureau for Astronomical Telegrams - Minor Planet Center, Cambridge.

Handling Editor: Paul Roggemans

The United Kingdom fireball of 30th March 2013: Observation and analysis using NEMETODE and visual data

William Stewart [1] *and Alex R. Pratt* [2]

This paper describes the fireball that was observed across England, United Kingdom at $00^{h}39^{m}$ UTC on 2013 March 30. The observations and subsequent analysis from NEMETODE, a network of low-light video cameras operated from Cheshire and West Yorkshire, are discussed as are visual observations submitted to online sources and periodicals. The method by which a correction to the observed magnitude derived from the video data is described and estimates are given of the radiant position, the path through the Earth's atmosphere and the orbital elements of the meteoroid. A speculative mass, size and origin of the meteoroid are given.

Received 2013 April 29

1 Introduction

During the early hours of Saturday, 2013 March 30, multiple postings began to appear on the Twitter social networking service indicating that a fireball had been seen over the UK. In subsequent hours further reports were logged on various online forums. These indicated that in spite of the poor weather over substantial parts of the country, the fireball had been widely observed. During a review of data later that day the authors, William Stewart (WS) and Alex R Pratt (ARP), noted that two NEMETODE cameras had captured a fireball at a time consistent with the visual reports.

2 NEMETODE Equipment and Methods

William Stewart operates three Watec 902H cameras with Computar aspherical 8 mm $f/0.8$ lenses, one facing North, one facing North-East and the other facing South-East from Ravensmoor, Cheshire. Alex R. Pratt operates a Watec 902H2 camera with a Computar aspherical 3.8 mm $f/0.8$ lens facing South from Leeds, West Yorkshire. William Stewart and Alex R. Pratt both run their cameras every night, irrespective of forecast conditions, in order to maximise the number of meteors captured.

Meteors are detected and recorded by UFO Capture (SonotaCo, 2005) running on Windows PCs; each capture is displayed to 0.1 s (processed internally to 0.04 s), time-synchronised to an NTP server. The resultant captures are processed by UFO Analyser (SonotaCo, 2007), registering against the Sky 2000 star catalogue with average positional errors of < 0.3 pixels and $< 0.03°$, to determine shower membership. The Ravensmoor and Leeds cameras operate across a baseline of 107 km and multi-station events are processed by UFO Orbit (SonotaCo, 2009) to estimate radiants, start and end heights, geocentric velocities and orbital elements. For this analysis SonotaCo, the author of the UFO software suite, analysed NEMETODE data using the prototype software tool he has developed known as "Fireball Inspector" (FBI). Further details relating to NEMETODE can be found on the authors' website (`http://www.nemetode.org/`).

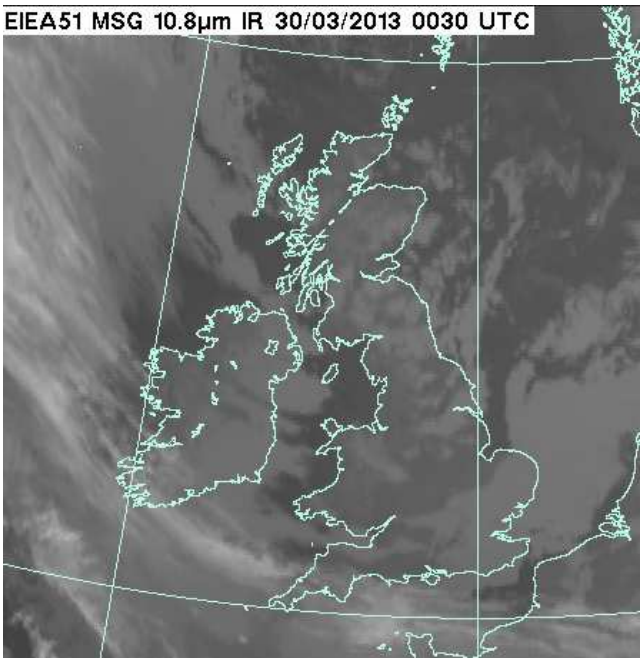

Figure 1 – Infra-red weather satellite image of the British Isles nine minutes before the fireball occurred.

3 Observing Conditions over the British Isles

Figure 1 shows the infra-red satellite view of the British Isles at $00^{h}30^{m}$ UTC on 2013 March 30, nine minutes before the fireball was observed[1]. Extensive cloud cover is evident over England with breaks from the Bristol Channel in the West, through the Midlands and towards The Wash in the East. The break in the clouds also extended North-West from the Midlands up towards Manchester and Liverpool then further North towards Cumbria. Some parts of Yorkshire are clear while others have broken cloud. At the time of the fireball, the waning gibbous Moon (91% illuminated) was in the South-South-East at an elevation between 14° and 18° as seen from most of England. Taking account of atmospheric extinction, the apparent magnitude of the Moon would have been approximately −11.5.

[1]West View Cottage, Swanley Lane, Ravensmoor, Nantwich, Cheshire CW5 8PZ, United Kingdom
Email: `ws@nemetode.org`
[2]76 Latchmere View, Leeds LS16 5DT, United Kingdom
Email: `arp@nemetode.org`

IMO bibcode WGN-416-stewart-fireball
NASA-ADS bibcode 2013JIMO...41..190S

[1]`http://www.metoffice.gov.uk/`

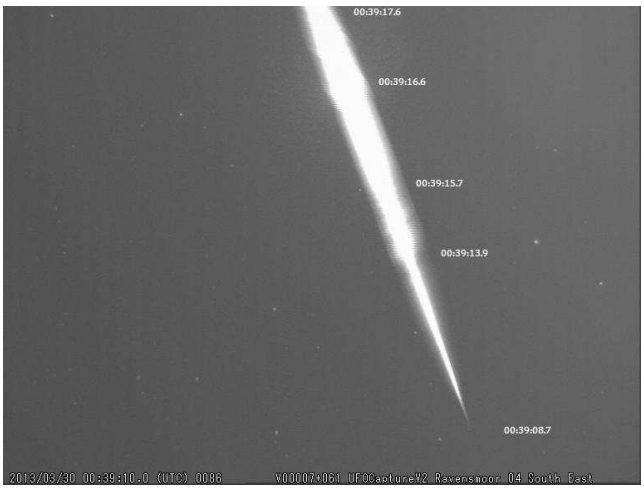

Figure 2 – Composite image of the fireball from the Ravensmoor South-East camera annotated with UTC time-markers. For operational reasons the camera has been rotated clockwise through 90° within its housing so what appears to be the bottom of the field of view is actually the left hand side. The "keystone" asterism in Hercules is visible in the lower half of the image, just to the left of centre.

Figure 3 – Composite image of the fireball from Leeds with the Moon illuminating the clouds in the lower left.

4 Observation from Ravensmoor

The sky was clear and the faintest stars detectable in the real time video were between magnitude 4.5 and 5.0. The first detection of the fireball was by the Ravensmoor South-East facing camera at $00^{\rm h}39^{\rm m}08\overset{\rm s}{.}7$ (all times given are UTC; NEMETODE timing accuracy is ±0.1 s). Figure 2 shows a composite image of the fireball. The fireball continued to pass through the Field of View (FOV) and exited at $00^{\rm h}39^{\rm m}17\overset{\rm s}{.}6$ (total duration of 8.9 s) leaving a wake that persisted for a further 0.3 seconds. No colours were determined as the camera system is black and white. The video of this fireball can be viewed on the authors' website.

5 Observation from Leeds

The sky had approximately 80% cloud cover and only one star was visible on the real-time video. The first detection of the fireball from Leeds was at $00^{\rm h}39^{\rm m}13\overset{\rm s}{.}0$ as it passed into a gap in the clouds (see Figure 3). It traversed the gap and passed behind another cloud at $00^{\rm h}39^{\rm m}14\overset{\rm s}{.}4$ before momentarily reappearing through very small cloud gaps at $00^{\rm h}39^{\rm m}15\overset{\rm s}{.}5$, $00^{\rm h}39^{\rm m}17\overset{\rm s}{.}1$ and $00^{\rm h}39^{\rm m}17\overset{\rm s}{.}8$.

No colours were determined as the camera system is black and white. The video can be viewed on the authors' website. During the same evening, prior and subsequent to the fireball, four other meteors were observed using this same system. Between 5 and 9 reference stars were visible in these captures. The camera system is permanently mounted and is not changed from one night to the next. On clear nights the number of reference stars is in excess of 20. The authors therefore conclude that triangulation data based on this observation is valid, in spite of the presence of just one reference star on the Leeds' fireball video.

6 Visual Observations

Visual observations were submitted by members of the public to various online forums including Stargazers Lounge[2], the Armagh Observatory Fireball Reports Database[3] and the Latest Worldwide Meteor / Fireball Reports Blog[4]. An observation was also submitted to "The Astronomer" (Hill, 2013). Where possible the authors contacted observers for additional follow up information however in the majority of cases this was not attempted as contact information for many of the submitters was not published.

A particularly detailed description was given by the experienced astronomical observer and founder of the Todmorden Astronomy Centre Peter Drew (PD) who observed the fireball from Bacup, Lancashire (53°42′ N, 02°12′ W)[1] (Drew P., personal communication):

"I was awake at 12.40am when I saw the fireball appear in full flight from the E side of a large Velux window that faces just E of S. It was relatively slow moving with a pure white head and a short fan shaped tail which contained orange and green hues. I sat up quickly enough to see it carry on westwards and gradually fade to nothing, there was no apparent after trail. The trajectory was pretty much parallel to the horizon and passed around 10 degrees above the Moon. The magnitude was at least −8 based on observations of Iridium flares, the observation lasted about 3 seconds during which the fireball covered around 30 degrees azimuth from 170° *to just over* 200°*."*

Another experienced observer, Christopher Hill (CH), also observed the fireball from Cheadle (53°24 N, 02°13 W), Greater Manchester (Hill, 2013; Hill C., personal communication):

"I was out observing Saturn at 00:40 GMT when I saw a bright fireball. Observing conditions were freezing cold but clear, some mist patches, still air at ground

[2] `http://tinyurl.com/oy4hfl2` and `http://tinyurl.com/q5xr2wo`
[3] `http://arpc65.arm.ac.uk/cgi-bin/fireballs/browse.pl`
[4] `http://thelatestworldwidemeteorreports.blogspot.jp/`

level but east wind high up, bright Moon nearby. Initially noticed fireball at an azimuth of approximately 150° *and it travelled slowly at* 5°/*s at an elevation of* 30°*, parallel to the horizon, dipping slightly. Brightness remained constant before dropping suddenly to extinction at an azimuth of* 180°*, to the west of Spica (confirmed via local known topography). The fireball was brighter than Venus at maximum though not as bright as the brightest Iridium flares the proximity to the moon made magnitude judgement challenging but estimate it to have been at least* −5*. No shadow observed though the bright moonlight would likely have drowned it out. The fireball had a very distinct orange (as opposed to white) head with orange sparkles falling away from it, somewhat reminiscent of a firework. No sound and no smoke trail."*

7 Other Potential Data Sources

The authors checked other potential online resources for observations with some limited success. There are no reports of this event logged on the American Meteor Society (AMS) website[5]. At the time of the fireball the all-sky cameras of the University of Hertfordshire[6] located at Bayfordbury and Exmoor were experiencing 100% cloud-cover as were the Church Crookham and Clanfield 2 cameras of the UK Meteor Observation Network (UKMON)[7] (Campbell-Burns P., personal communication). A search for "fireball" or "meteor" on the online photo sharing website Flickr[8] for the date of the fireball, a strategy which has proved useful in the past, also proved fruitless. The Met Office (The UK's National Weather Service) checked weather radar data but saw no evidence of an object entering the earth's atmosphere at the time of the event.[1]

Michael Morris (MM), observing from a location 0.8 km North-North-East of the city of Worcester in the West Midlands (53°12′ N, 02°13′ W) with a Samsung SDC 435 low light video camera equipped with 2.1 mm lens, obtained a video of the early stages of the fireball[2,9] (Morris M., personal communication). North is to the top and East is to the left of the FOV. Being an internal reflection of the Moon, the bright object in the upper right is 180° out of position. Michael Morris has stated that the time code is accurate to ±2 seconds. The time code as the fireball first becomes visible is $00^{\mathrm{h}}39^{\mathrm{m}}06\overset{\mathrm{s}}{.}7$. Based on the duration and brightening of the object as it exits the FOV at $00^{\mathrm{h}}39^{\mathrm{m}}10\overset{\mathrm{s}}{.}6$, the authors believe that this video does not show the fireball at its brightest.

The same video system was used to capture a 77° elevation pass of the International Space Station (ISS) later that night[10], a pass for which the estimated maximum brightness was magnitude -3.5[11].The authors have compared the two videos and it is clear that observing conditions were better for the pass of the ISS compared to those for the time of the fireball. In spite of this, the early stages of the fireball are significantly brighter than the ISS. The authors conservatively estimate the difference to be 1 magnitude brighter. The ISS passed close to the centre of the FOV whereas the fireball was close to the edge. Vignetting from a 2.1 mm lens would be expected to make objects close to the edge of the FOV appear dimmer but the impact of this has not been quantified and a correction factor not applied. Michael Morris has also confirmed that the fireball appears *"...much brighter than Jupiter is when it appears in a video..."* (Morris M., personal communication). At opposition, Jupiter has a maximum magnitude of −2.9. The authors therefore conclude that the initial stages of the fireball had an observed magnitude of at least −4.5.

8 Trajectory Analysis

Having processed the Ravensmoor and Leeds data through UFO Analyser, the authors attempted to determine key parameters relating to the velocity, the atmospheric trajectory and orbital elements of the meteoroid using UFO Orbit. The software classified this as a Q1 event i.e. the data is only of sufficient quality to meet minimum conditions for normal radiant computation. This is most likely due to the cloud cover affecting the Leeds observation. Although a reasonable ground track and orbit could be determined using this software, the authors had concerns relating to the derived deceleration values during the object's path through the atmosphere. These concerns were discussed with the software developer, SonotaCo, who in turn offered the use of a new tool that he has developed (though not publically released) called "Fireball Inspector" (FBI) (SonotaCo, personal communication). This tool has been designed for the precise measurement of fireballs and can adjust for timing errors and errors in radiant direction and entry point. The authors provided their data to SonotaCo for analysis with FBI v1.02.

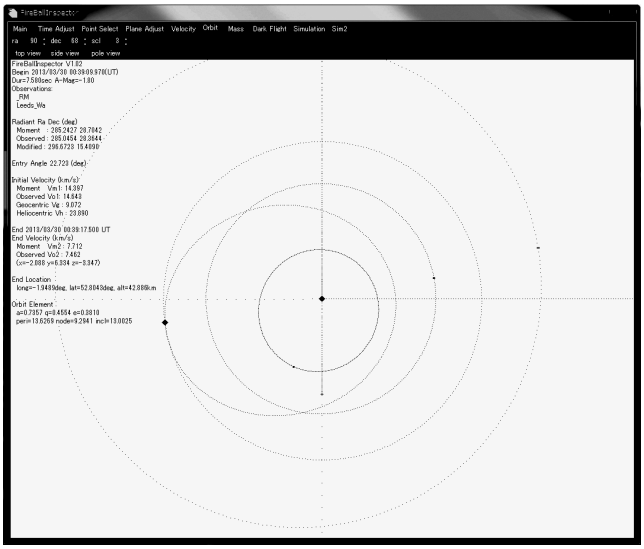

Figure 4 – FBI orbit estimate (courtesy SonotaCo).

[5] http://www.amsmeteors.org/fireball_event/2013/
[6] http://star.herts.ac.uk/allsky/about.php?c=1
[7] http://ukmeteornetwork.co.uk/
[8] http://www.flickr.com/
[9] http://www.youtube.com/watch?v=zdnoPoAQ1J0
[10] http://www.youtube.com/watch?v=UBuY3TOkMYo
[11] http://www.heavens-above.com

Table 1 – FBI estimate for the orbital elements of the meteoroid (courtesy SonotaCo).

a (AU)	q (AU)	e	ω (°)	Ω (°)	i (°)
0.74 ± 0.07	0.46 ± 0.13	0.38 ± 0.12	13.6 ± 10.6	9.29 ± 0.0	13.00 ± 10.0

The timing adjustment works by matching the light curves from the two separate observers. Unfortunately this was not possible as the cloudy conditions in Leeds prevented a light curve being generated that could be matched to the Ravensmoor observation.

SonotaCo's analysis indicates that the instantaneous radiant direction (direction at the time of entry point ignoring the effects of the Earth's rotation, movement and the effect of gravity) was RA 285.24°, DEC +28.70°. The instantaneous entry velocity was 14.4 km/s and the observed velocity was 14.6 km/s. This allows an orbit for the meteoroid to be estimated as shown in Table 1 and Figure 4.

As shown in Figure 5, the velocity remained reasonably constant for 5 seconds before slowing down to 7.7 km/s at the end of the Ravensmoor video. This velocity figure is significantly different from that determined by UFO Analyser. SonotaCo believes this is a consequence of the small cross angle Q_c (3.6°) between the two observing sites; that the FBI software has provided a significant correction and that the revised figure of 7.7 km/s is much more accurate (SonotaCo, personal communication).

Figure 6 shows (in light grey) the derived ground track as determined by SonotaCo's FBI software. The trajectory adjustment converged to a reasonable result with the first data-point (at $00^{\rm h}39^{\rm m}09\overset{\rm s}{.}6$) being an altitude of 83.2 km at 53°04′ N, 00°36′ W. The authors note that the first evidence of the fireball on the video sequence was at $00^{\rm h}39^{\rm m}08\overset{\rm s}{.}7$ and that the first 3 seconds of data commencing $00^{\rm h}39^{\rm m}09\overset{\rm s}{.}6$ in Figure 5 show reasonably constant values for the velocity and the rate of decrease in altitude. They have therefore extrapolated backwards in time to $00^{\rm h}39^{\rm m}08\overset{\rm s}{.}7$ in order to estimate the position of the meteoroid at the time it first became apparent on the video. An entry altitude of 88.3 km is estimated at 53°05′ N, 00°25′ W which is approximately 17 km South-South-East of the city of Lincoln in Lincolnshire, UK.

The entry angle was 67.2° to the zenith. The fireball continued on a bearing of 252.8°, passed directly over the city of Nottingham, carried on just to the South of Derby before exiting the Ravensmoor South-East FOV at 52°48′ N, 01°57′ W by which time the altitude had dropped to 42.8 km. This location is approximately 17 km South-East of the town of Stone in Staffordshire. This equates to an observed ground track length of 107.4 km and an atmospheric path length of 116.3 km.

As the meteoroid continued on its trajectory the velocity would decrease until it was below the threshold for atmospheric ionisation (circa 2 – 4 km/s) after which the fireball would no longer be visible even as it continued to travel downrange. Christopher Hill was closer to the ground track than Peter Drew (65 km compared to 100 km) and so his extinction azimuth estimate may have less uncertainty. However his extinction azimuth estimate was closer to the bright moon and so it may have been more challenging to see the fainter part of the trail against a relatively bright background.

While the authors have confidence in that part of the trajectory captured on video, the remainder of the meteoroid's path (shown in black in Figure 6) is speculation. SonotaCo in particular cautions against reading too much into this part of the plot as the potential flight path after the object left the Ravensmoor FOV is based on a number of assumptions: that atmospheric density was typical for each altitude, that there were no winds and that the residual mass of the object was 0.1 kg. For reference, the weather conditions at the closest weather station to this part of the trajectory (Shawbury, Shropshire at a distance of 12 km) reported the following for 00:50 UTC on 2013 March 30[12]: Conditions: −2°C, Partly Cloudy; Humidity: 76%; Visibility 10 km; Pressure 1010.84 mb steady; Wind: N 10 km/h.

[12] `http://uk.weather.com`

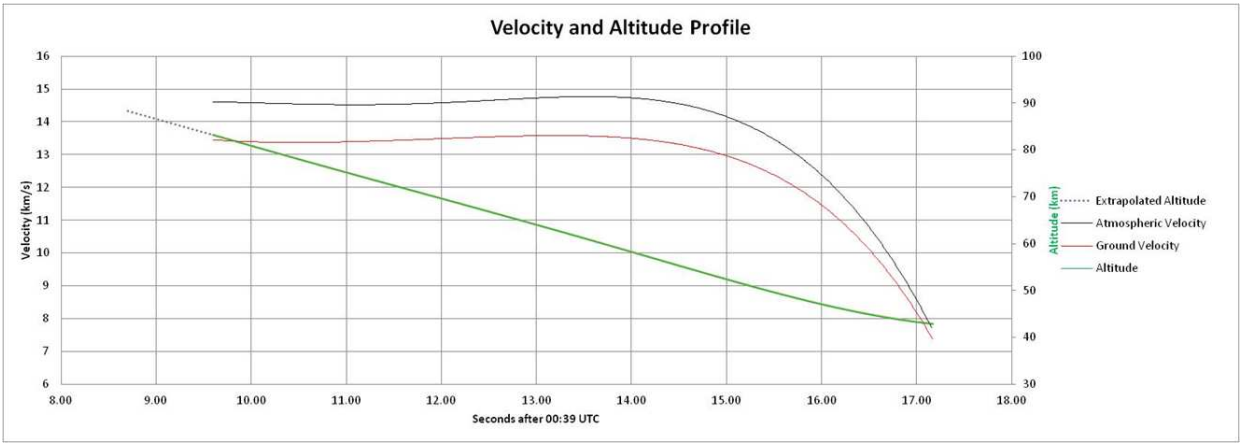

Figure 5 – Velocity and Altitude plots (data courtesy of SonotaCo).

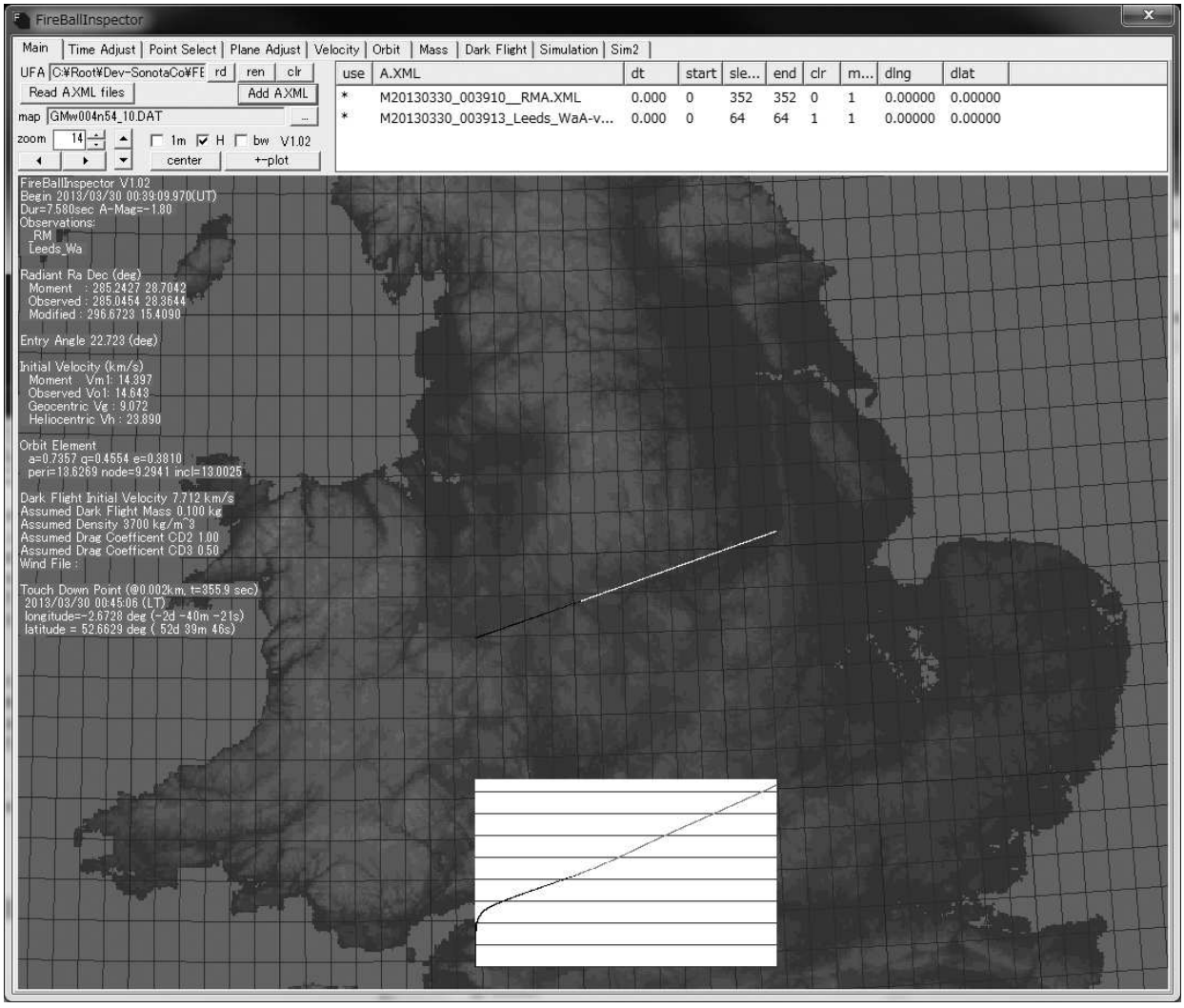

Figure 6 – FBI Ground track and altitude profile (courtesy SonotaCo).

Had there been a surviving object (or fragments thereof) they would have come down somewhere within a distribution or dispersion ellipse, the semi-major axis of which would be aligned with the trajectory. A touchdown point of 52°40′ N, 02°40′ W is given which lies approximately 7 km to the SE of Shrewsbury in Shropshire. This position lies on a bearing of 195.5° from Peter Drew's observing location and is approximately 12 km up-range from the point on the ground-track given by his extinction estimate of "just over 200°". From Christopher Hill's observing location the bearing of the touchdown point is 201.1° which is approximately 32 km downrange from his stated fireball extinction azimuth of 180°.

Based on typical densities, a 0.1 kg object would have a radius in the region of 20 mm. Due to the small size, the uncertainties in the extinction azimuth, assumptions in the analysis and the terrain in the vicinity of the touchdown point, the authors have not attempted to recover any fragments, should any fragments have survived down to the Earth's surface.

9 Observed Magnitude

The authors have been able to extract magnitude data from the Ravensmoor South-East video sequence between $00^{h}39^{m}09^{s}.5$ and $00^{h}39^{m}17^{s}.3$ using UFO Analyser (SonotaCo, 2007). There are some gaps in the data, particularly between $00^{h}39^{m}13^{s}.2$ and $00^{h}39^{m}15^{s}.2$ due, it is suspected, to limitations in the video system's ability to record very large and rapid fluctuations in brightness. Some magnitude data is also missing from the start and end of the trail. Variations in magnitude are apparent from Figure 2 and can also be seen in the video sequence on the author's website.

The observed magnitude is denoted by the solid black line in Figure 8. Attention is drawn to the observed magnitude (left hand) scale. Estimates of the magnitude of the meteor from visual observers are much higher than that indicated by the scale on the graph. There are a number of contributing factors to this, one of which is that the camera used, a Watec 902H, has an 8 bit sensor and therefore has 256 brightness detection levels. The camera system has been optimised for sensitivity to very faint meteors and as a consequence when very bright events occur, the CCD pixels become saturated. Another factor is that the algorithm implemented in UFO Analyser determines observed magnitude by comparing the brightness of the transient event (in this case the fireball) with the brightness of the reference stars within the FOV. In order to reject the effect

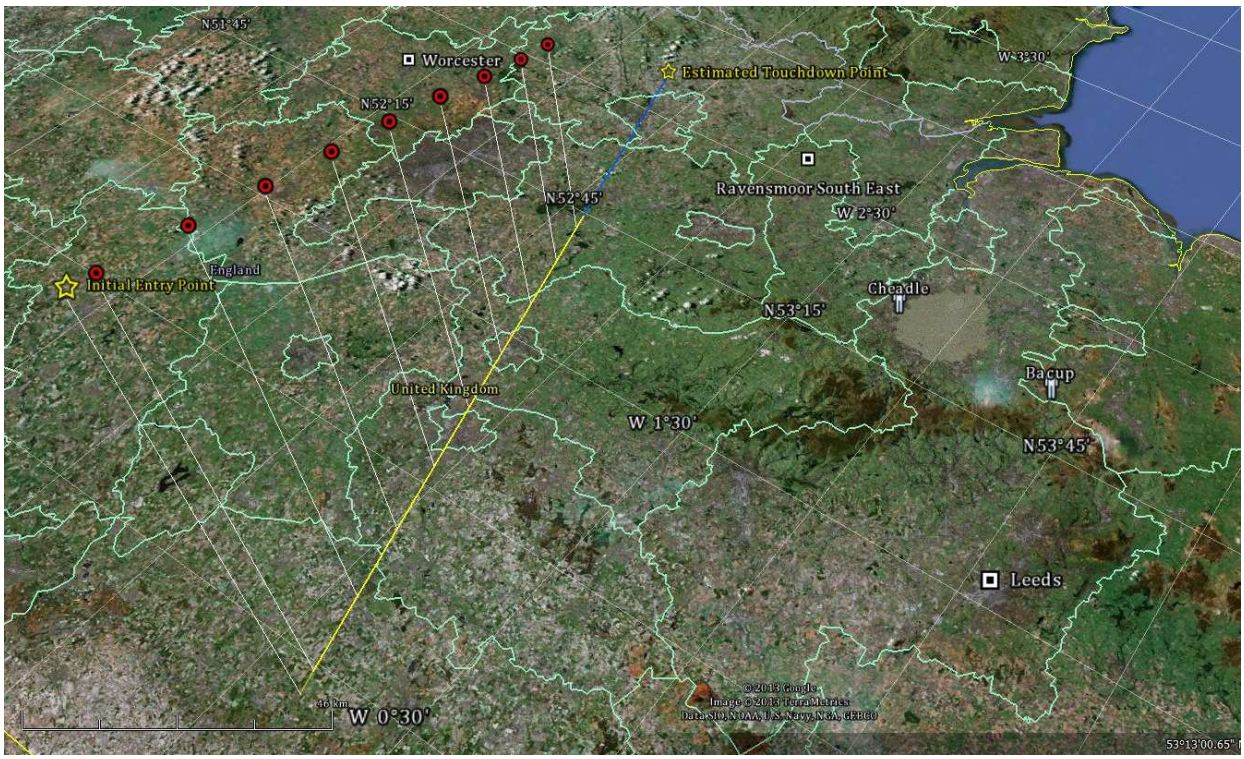

Figure 7 – Annotated ground track based on SonotaCo analysis of NEMETODE data and visual observations from an altitude of 200 km looking South-West. The red dots are time-markers for seconds with the first one after Initial Entry Point being $00^{\mathrm{h}}39^{\mathrm{m}}10^{\mathrm{s}}$ UTC on 2013 March 30.

of afterglow, the algorithm ignores those pixels that do not change in value in successive frames. This fireball was very bright and had a very low angular speed across the FOV – as a consequence the algorithm ignored the saturated pixels and hence underestimated the observed magnitude (SonotaCo, personal communication). Only the observed magnitude is underestimated, the magnitude variation data is still valid.

It is clear from Figure 6 and Figure 7 that the meteoroid's trajectory was taking it towards the Ravensmoor South-East camera. If the fireball had maintained a constant luminosity then the observed magnitude at Ravensmoor would therefore increase. It is also clear from Figure 2 that the observed elevation was increasing and from Figure 5 that the meteoroid altitude was decreasing. Both of these would reduce the dimming due to atmospheric absorption. Corrections were therefore applied in order to determine the absolute magnitude at each stage in the trajectory.

The magnitude at a distance of 100 km was calculated using the formula:

$$m_{100} = m_{obs} - (2.512 \log L_{inc}) \qquad (1)$$

where m_{100} is magnitude at a distance of 100 km, m_{obs} is the observed magnitude and L_{inc} is the increase in luminosity given by the formula:

$$L_{inc} = (\frac{d}{100})^2 \qquad (2)$$

where d is the distance (in km) between the observer and the meteoroid. The air mass along the observation line of site was estimated using the Rozenburg equation:

$$\text{Air Mass} = \frac{1}{\cos z + 0.025\mathrm{e}^{(-11\cos z)}} \qquad (3)$$

where z is the zenith angle (Rozenberg, 1966). Each air mass was assumed to lead to a reduction in magnitude of 0.28. As the decrease in vertical distance between the meteoroid and the observer was due to the meteoroid losing (as opposed to the observer gaining) altitude, the magnitude reduction factor of 0.28 was used for all calculations.

The absolute magnitude is denoted by the solid grey line in Figure 8. As expected, the variation in magnitude between maximum and minimum has been reduced, in this case from 2.5 to 1.5.

Many visual observers commented on the brightness of the object with some comparing it to that of the Moon or the ISS. The authors have taken account of these reports[3,4] and, based on observer locations and the trajectory, determined an average absolute magnitude of −10. However, these reports were more likely to be submitted by members of the public as opposed to astronomers and, as already noted, even experienced observers can reach different conclusions when attempting to quantify just how bright an object is, particularly when it occurs unexpectedly. In the absence of a range of reference objects it is not possible to say that an object was brighter than X but fainter than Y. Experience, the relatively large size and the slow angular speed can all contribute to an over-estimate of the brightness and for this reason the authors urge caution when attempting to draw conclusions from these estimates. Peter Drew estimated the maximum magnitude to be *"... at least −8 ..."* while Christopher Hill estimated it to be *"... at least −5 ..."*. Applying equations (1), (2) and (3) for the meteoroid's estimated position at $00^{\mathrm{h}}39^{\mathrm{m}}15\overset{\mathrm{s}}{.}0$ leads to an absolute magnitude estimate

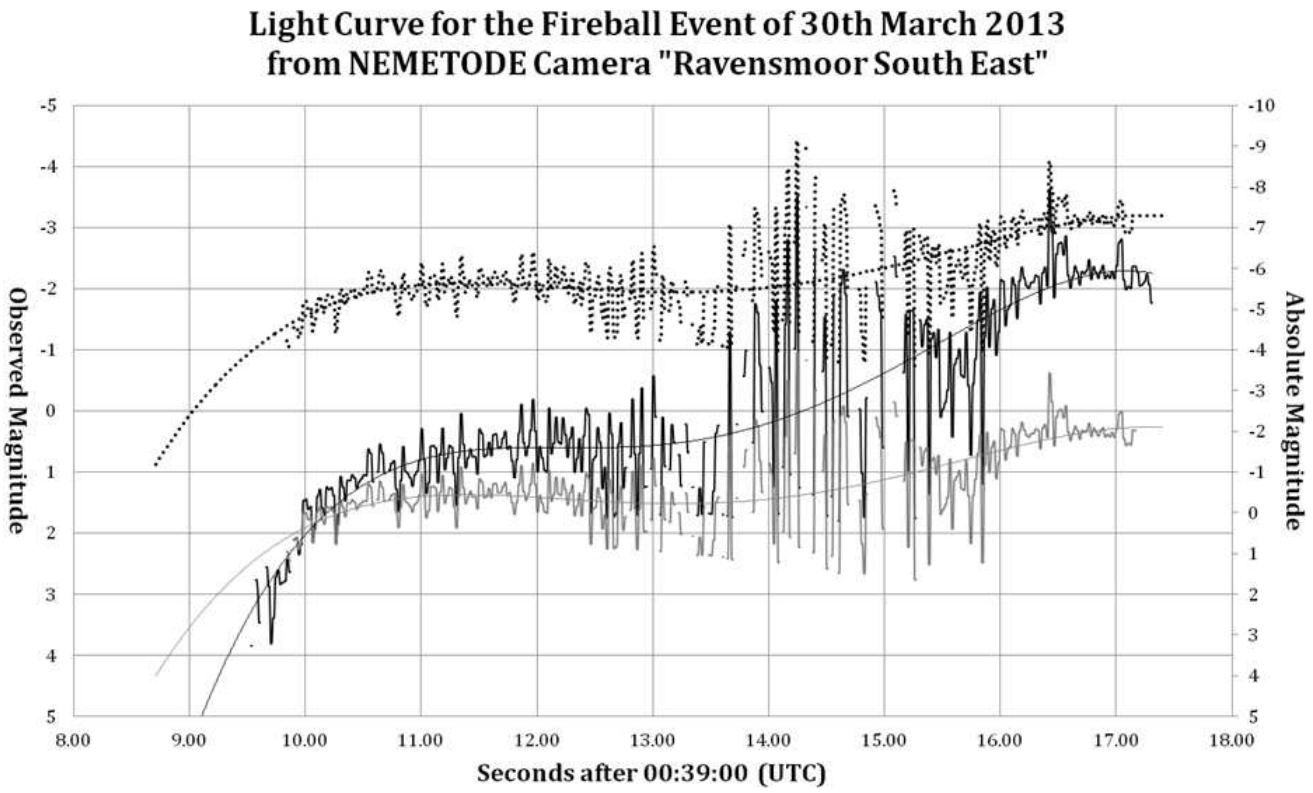

Figure 8 – Observed Magnitude (solid black line) extracted from the Ravensmoor South-East video sequence. The solid grey line is the Absolute Magnitude, taking account of distance and atmospheric extinction. The dotted black line is a scale adjustment of the Absolute Magnitude, correcting for the magnitude under-estimate in the original NEMETODE data.

of at least −8.8 for Peter Drew's observation and −5.2 for Christopher Hill's observation. Obviously there is a significant difference in these two values. Christopher Hill's observing location would have placed the fireball's path across the sky closer to the Moon but in the absence of additional information, it is difficult to draw any firm conclusions other than to place a lower limit of −5.0 on the maximum absolute magnitude.

The author's assertion that the Michael Morris video only showed the early stages of the fireball is further reinforced by noting that the fireball left the FOV of the Worcester camera no later than $00^{h}39^{m}12^{s}.6$ (time-code of $00^{h}39^{m}10^{s}.6$ ±2 s). Comparing this against Figure 8 (bearing in mind that Michael Morris timing data is accurate to ±2 s whereas NEMETODE timing data is accurate to ±0.1 s), it can be seen that this was prior to the fireball reaching its greatest magnitude. In order to convert the observed magnitude estimate of at least −4.5 into an absolute magnitude estimate, equations (1), (2) and (3) were applied for the meteoroid's estimated position at $00^{h}39^{m}12^{s}.6$ and an absolute magnitude estimate of at least −5.5 obtained for this early stage of the fireball. Applying the correction earlier (when the meteoroid was further from the observer) leads to an increase in the absolute magnitude estimate of 0.2 magnitudes per second (i.e. at $00^{h}39^{m}10^{s}.6$ the absolute magnitude estimate rises to −5.9).

As can be seen from the solid grey line in Figure 8, the Ravensmoor data shows the early stages of the fireball having an absolute magnitude of approximately −0.5. For reasons already discussed, this is known to be an under-estimate. By making use of the absolute magnitude estimate for the early stages of the fireball from the analysis of Michael Morris's data, a correction can be applied to the absolute magnitude for the Ravensmoor data to scale the absolute magnitude of the early stages of the fireball to match that obtained from the analysis of the Michael Morris data. The dotted black line on Figure 8 has this scale adjustment applied.

Having combined all these observations the authors conclude that the absolute magnitude was in the range −5 to −9 and, based on the available video evidence, suggest that an absolute magnitude of -7 ± 1 is a reasonable estimate.

10 Magnitude Variations from Ravensmoor Video Data

Commencing $00^{h}39^{m}09^{s}.5$, the first 1.5 seconds show a steady rise in brightness from observed magnitude +3.3 to +0.5 after which it remained reasonably constant for 2.5 seconds. Commencing $00^{h}39^{m}13^{s}.9$ there is a series of flickers / flashes accompanied by a brightening to an average observed magnitude of −0.8 with spikes to −2 and −3. This is accompanied by a broadening of the width of the fireball (see Figure 2). From $00^{h}39^{m}15^{s}.7$ the flickers / flashes stop but the observed magnitude continues to increase to an average maximum of −2.7 before reaching a plateau then decreasing slightly after $00^{h}39^{m}17^{s}$.

The video evidence suggests that the fireball had reached maximum brightness and was beginning to fade as it exited the FOV of the Ravensmoor South-East camera. Many of the visual observations mention that

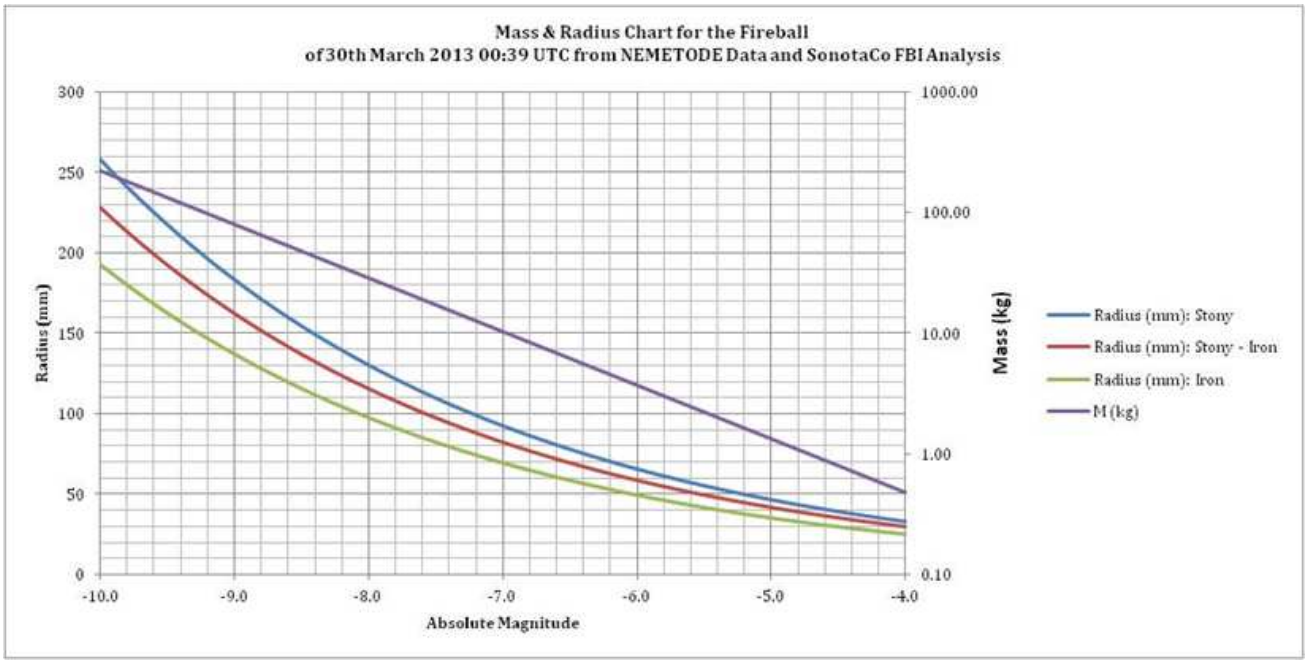

Figure 9 – Radius and Mass plot based on Jacchia's formula for the derived V_g and z from SonotaCo Data. Typical densities for Stony, Stony-Iron and Iron meteorites are assumed to be 3.2, 4.5 and 7.5 g/cm^3 respectively.

the object faded from view but it is not clear how abruptly this occurred. Christopher Hill mentioned that the *"Brightness remained constant before dropping suddenly to extinction..."* whereas Peter Drew stated that it *"...gradually fade[d] to nothing..."*.

11 Fragmentation and Tail Development

There is a suggestion in Figure 2 and from the visual reports that during the course of the event a tail developed. Peter Drew described it as being "fan shaped" this may explain the significant broadening of the trail seen in the Ravensmoor data after $00^{\rm h}39^{\rm m}13\overset{\rm s}{.}9$.

At least three visual observers mentioned fragmentation or parts falling away in their reports[4] (Hill C., personal communication). It is reasonable to suggest that commencing $00^{\rm h}39^{\rm m}13\overset{\rm s}{.}9$ there was a fragmentation event (characterised by the aforementioned flickers / flashes) that gave rise to multiple trails that were too close together to be individually resolved by the NEMETODE cameras. As these fragments are likely to have a range of masses and cross sections, they would likely decelerate at different rates and a broad tail would develop. As can be seen from Figure 5, significant deceleration commenced at $00^{\rm h}39^{\rm m}14^{\rm s}$.

Observer used many colours to describe the tail – predominantly orange and green but also red, yellow, blue and purple. It is not clear if these colours are due to the excitation of and subsequent photon emission from particular species of atmospheric gases or whether they are indicative of the meteoroid's chemical composition.

The authors have compared the data in Table 1 with the observation that the object was able to penetrate the atmosphere to an altitude of approximately 60 km (see Figure 5 and Figure 8) before undergoing the presumed fragmentation event. Taken together, this suggests that the meteoroid was possibly asteroidal in origin and the authors note that the orbital parameters bear some similarity to those of the Apohele family of Interior Earth Objects.

12 Meteoroid Size

Jacchia's formula for maximum visual magnitude

$$m_v = 4.84 - 2.25 \log M - 8.75 \log V_g - 1.5 \log \cos z \quad (4)$$

may be used to estimate the mass of a meteoroid from the maximum absolute magnitude where m_v is the maximum absolute magnitude, M is the original meteoroid mass, m_g is the geocentric velocity and z is the zenith angle (Jacchia et al., 1967). Figure 9 shows a plot of Radius and Mass against Absolute Magnitude for $V_g = 14.5$ km/s and $z = 67.2°$. Assuming a maximum absolute magnitude of -7, the authors estimate that the meteoroid had an original mass of the order of 10 kg and a radius of the order of 80 mm.

13 Conclusions

From a combination of visual and video observations the authors conclude that at $00^{\rm h}39^{\rm m}08\overset{\rm s}{.}7$ UTC on 2013 March 30 a meteoroid of approximate mass 10 kg and radius 80 mm entered the earth's atmosphere at an altitude of 83 km and a zenith angle of 67.2° over Lincolnshire in the UK, producing a fireball with a duration of at least 8.9 seconds and an absolute magnitude of the order of -7. The fireball proceeded on a West-South-West trajectory over Nottinghamshire at approximately 14.5 km/s before fragmenting at an altitude of 60 km, rapidly decelerating and continuing over Derbyshire, Staffordshire and (in all likelihood) Shropshire. An estimate of the orbital elements suggests that the meteoroid may be related to the Apohele family of

Interior Earth Objects. The use of online social and reporting tools has been demonstrated to be of value in locating supplementary information to aid this type of analysis.

14 Acknowledgements

The authors are deeply indebted to SonotaCo for analysing their data with the Fireball Investigator tool. Without his knowledge and insight, much of this paper would not have been possible. Thanks are also due to Peter Drew and Christopher Hill for their detailed visual observations and to Michael Morris for the use and analysis of his video – all of which have helped support some of the conclusions drawn in this paper. Finally thanks is also offered to Bill Ward for setting up the Meteor Observer's Forum[13] through which the NEMETODE group was formed. Co-author Alex R. Pratt thanks Len Entwisle for introducing him to SonotaCo's program suite and Bill Ward for initial assistance with the software.

[13] `http://meteorobserver.proboards.com/index.cgi`

References

Hill C. (2013). "Meteor & fireball notes". *The Astronomer*, **49**, 322.

Jacchia L. G., Verniani F., and Briggs R. E. (1967). "Selected results from precision-reduced superschmidt meteors". *Smithsonian Contributions to Astrophysics*, **11**, 1–7.

Rozenberg G. V. (1966). *Twilight: A Study in Atmospheric Optics*. Plenum Press, New York, 160 pages.

SonotaCo (2005). "UFO Capture V2". `http://sonotaco.com/soft/e_index.html` .

SonotaCo (2007). "UFO Analyzer V2". `http://sonotaco.com/soft/e_index.html` .

SonotaCo (2009). "UFO Orbit V2". `http://sonotaco.com/soft/e_index.html` .

Handling Editor: Paul Roggemans

η Aquariids outburst 2013 observed by CAMS

Carl Johannink [1]

The Dutch CAMS Network registered several η Aquariids some of which were captured during the activity outburst of the η Aquariids in 2013.

Received 2013 May 17

1 Introduction

The η Aquariids are one of the most difficult observable major meteor streams of the Northern hemisphere. Just in the early twilight some of these shower members associated with the October Orionids may be noticed. In 2008 this meteor stream could be successfully observed from the Netherlands (van Leuteren et al., 2008).

2 Results for 2013

Favorable weather circumstances without moonlight interference allowed the CAMS network in the Netherlands to run during each night. Two η Aquariid orbits could be derived from the CAMS stations at Hengelo (Martin Breukers) and at Alphen aan de Rijn (Robert Haas) in the nights of May 2 and 3.

The first few messages about a real outburst of this stream occurred on May 6, reported by Koen Miskotte, Michel Vandeputte and Peter van Leuteren. The same day all active CAMS stations assured the analyses of their data allowing the same day to identify and compute the double station meteors. Indeed double station η Aquariids were recorded by the 6 stations in the Netherlands. One double station η Aquariid was recorded by Martin Breukers (Hengelo) and Robert Haas (Alphen aan de Rijn), two other shower members by Piet Neels (Ooltgensplaat) and Klaas Jobse (Oostkapelle), one by Klaas Jobse in oostkapelle and Marco Langbroek in Leiden and finally three more by Koen Miskotte (Ermelo) and the author (Gronau). Figure 1 shows the radiant positions obtained for these 9 η Aquariids.

As there are a few days of time between the outburst of May 6 and the other two η Aquariids, the radiant positions were corrected for the radiant drift. A drift of +0.76 degrees per day in Right ascension and +0.422 degrees per day in declination was found in the literature (Jenniskens, 2006). The positions found for May 6 were taken as starting points. The result is shown in Figure 2.

For all 9 η Aquariids the orbits could be calculated. Figure 3 shows a plot of the inclination against the longitude of Perihelion (Π).

Except for the orbital elements i and 'Π' of the 9 orbits recorded by the CAMS some more values from literature were included. These values were taken from studies by Lindblad, Galligan and others (Jenniskens, 2006).

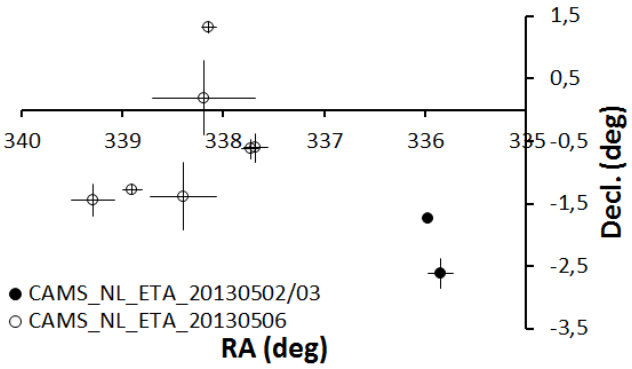

Figure 1 – Radiant positions of the 9 η Aquariids recorded by the CAMS-stations in the Netherlands.

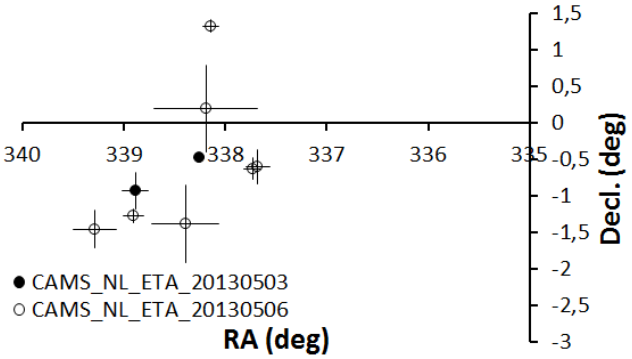

Figure 2 – Radiant positions for 9 η Aquariids corrected for the radiant drift (starting position = May 6).

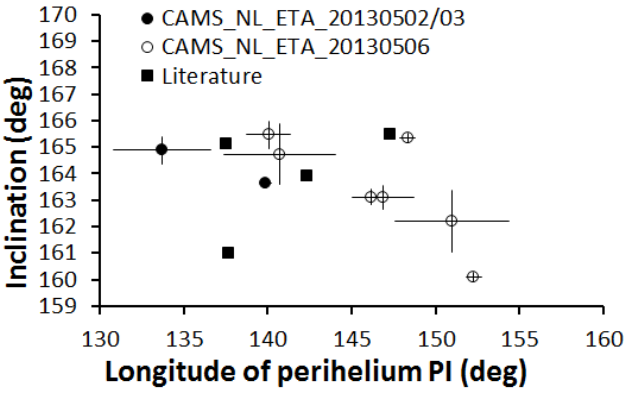

Figure 3 – Plot of the inclination against longitude of perihelion for the 9 recorded η Aquariids.

The values obtained by CAMS are in good agreement with the literature although some remarks should be made. The point at the extreme right ($\Pi \sim 151°$) concerns a double station η Aquariid by the stations Alphen aan de Rijn and Hengelo in the morning of 6 May with $V_g \sim 68$ km/s which is about 5% above the reference value of $V_g \sim 65$ km/s. Possibly the large dis-

[1]Carl Johannink, Schiefestr. 36, 48599 Gronau, Germany
Email: c.johannink@t-online.de

IMO bibcode WGN-416-johannink-eta2013
NASA-ADS bibcode 2013JIMO...41..199J

tance between the two stations ($\sim$ 150 km) may explain the poorer accuracy.

Further we have the point at $\Pi \sim 141°$ with a somehow larger error margin. This point represents a double station meteor from the stations Ermelo and Gronau. The geometry between these stations, their field of view (above the county of Kleve) and the radiant of the η Aquariids in the early morning is such that the angle of convergence remains smaller than 10 degrees. In this particular case the angle of convergence was 6.9 degrees. Such low values in angle of convergence increase the risks for larger error margins on the orbital elements.

Table 1 lists the orbital elements of the η Aquariids recorded by CAMS in the Netherlands. The values given by Lindblad (1990) are mentioned to compare.

The results however illustrate how powerful the CAMS software really is for the orbit computations to produce acceptable results in spite of the smaller angles of convergence.

3 Conclusions

The CAMS network in the BeNeLux recorded 9 double station η Aquariids and derived their orbital elements thanks to the favorable weather and the efforts of the participating stations at Alphen aan de Rijn (R. Haas), Ermelo (K. Miskotte), Gronau (C. Johannink), Hengelo (M. Breukers), Leiden (M. Langbroek), Ooltgensplaat (P. Neels), Oostkapelle (K. Jobse) and Wilderen (J.-M. Biets). The radiant positions and orbital elements fit well with the previously obtained data from the literature. However the quantity of data is still too small for any more detailed study.

Acknowledgments

A word of thanks to Peter Bus for his critical review of this paper and to Paul Roggemans for his translation work.

References

Jenniskens P. (2006). *Meteor Showers and their parent comets*. Cambridge University Press. (pages 705–706).

Lindblad B. A. (1990). *The orbit of the eta Aquariid meteor stream*. Asteroids, Comets, Meteors III. (pages 551–553).

van Leuteren P., Miskotte K., and Vandeputte M. (2008). "Observing reports". *eRadiant*, **4**, 74–82.

Handling Editor: Paul Roggemans

Table 1 – Orbital elements of the η Aquariids recorded by the CAMS stations Gronau (312), Hengelo (322), Oostkapelle (331/332), Ooltgensplaat (341), Ermelo (351), Alphen a/d Rijn (362) and Leiden (366).

Time (UT) May 2013	RA_{geo} [°]	DEC_{geo} [°]	V_g [km/s]	q [AU]	$1/a$ [1/AU]	i [°]	ω [°]	Ω [°]	Stations
2.12328	338.887±0.127	−0.927±0.245	65.197±0.762	0.53364±0.01636	0.0892±0.0649	164.873±0.509	92.021±2.893	41.6792±0.0027	362,322
3.09958	338.256±0.051	−0.478±0.062	66.244±0.089	0.56864±0.00213	0.0057±0.0080	163.630±0.122	97.268±0.332	42.6270±0.0004	362,322
6.09439	338.902±0.098	−1.269±0.089	68.115±0.130	0.59820±0.00328	−0.1620±0.0123	165.345±0.168	102.807±0.464	45.5279±0.0006	312,351
6.10061	338.189±0.510	0.195±0.590	68.569±1.074	0.61574±0.02187	−0.2168±0.1000	162.194±1.156	105.449±3.411	45.5364±0.0044	362,322
6.11028	338.394±0.331	−1.381±0.536	65.426±0.875	0.56288±0.01964	0.0984±0.0752	164.734±1.127	95.148±3.330	45.5439±0.0053	312,351
6.11063	339.287±0.215	−1.451±0.257	65.778±0.318	0.54999±0.00874	0.0447±0.0270	165.467±0.525	94.509±1.291	45.5436±0.0019	312,351
6.11334	337.680±0.120	−0.001±0.234	66.787±0.550	0.60130±0.01039	−0.0199±0.0499	163.098±0.437	101.340±1.837	45.5482±0.0024	341,332,331
6.11822	338.143±0.076	1.329±0.091	69.043±0.155	0.62027±0.00309	−0.2876±0.0145	160.085±0.182	106.727±0.472	45.5382±0.0005	331,366
6.11822	337.732±0.086	−0.001±0.154	66.602±0.297	0.59704±0.00647	−0.0040±0.0254	163.116±0.290	100.625±1.068	45.5529±0.0013	341,331
Lindblad (1990)	337.60	−1.60	65.90	0.61	0.03	165.50	101.50	45.80	

Preliminary results

Results of the IMO Video Meteor Network — August 2013

Sirko Molau[1], *Javor Kac*[2], *Stefano Crivello*[3], *Enrico Stomeo*[4], *Geert Barentsen*[5] *and Rui Goncalves*[6]

In 2013 August, cameras of the IMO Video Meteor Network recorded over 72 000 meteors in 9 100 hours of effective observing time. A detailed activity profile is presented for a one-week period centered at the maximum around $\lambda_\odot = 140°$, based on almost 50 000 Perseids the Network data recorded in 2011–2013. A new procedure for calculating the population index value from video observations is proposed, which takes advantage of the broad spectrum of limiting magnitudes for different cameras contributing flux measurements and does not require brightness data for individual meteors.

Received 2013 October 26

1 Introduction

August 2012 was truly a record-breaking month. Thanks to perfect observing conditions we recorded over 75 000 meteors in more than 10 500 hours of effective observing time – far more than in any month before (Molau et al., 2012). But also August 2013 was not bad. The weather was cooperative with most observers. 53 out of 71 operated cameras were successful in at least twenty and as much as 40 cameras in twenty-five and more observing nights. The number of cameras that did not miss a single night grew to six, distributed all over Europe: Bilbo and Stg38 (Italy), Templar1 and Templar3 (Portugal) as well as Remo1 and Remo3 (Germany).

If there were not three cameras less than last year, we probably had obtained the same result. With over 72 000 meteors recorded in 9 100 hours of effective observing time (Table 1 and Figure 1), it was just a few percent less.

Wolfgang Hinz has finished his relocation and his camera Acr resumed operation after a break of a few months just in time for the Perseids. It is observing now from Schwarzenberg in Saxony, Germany in the northern direction, so that the field of view is overlapping with the three southward facing cameras Armefa, Ludwig1 and Remo2 in the Berlin area.

Furthermore, we can welcome the third lady in the IMO Network. Jenni Donati from Italy is operating the camera Jenni. Even though her Mintron camera is equipped with a wide-angle lens of "only" $f/1.2$, Jenni could play in the "premier league" right from the start and contribute almost 2 000 meteor records in August.We keep our fingers crossed that she will be equally successful in the months to come.

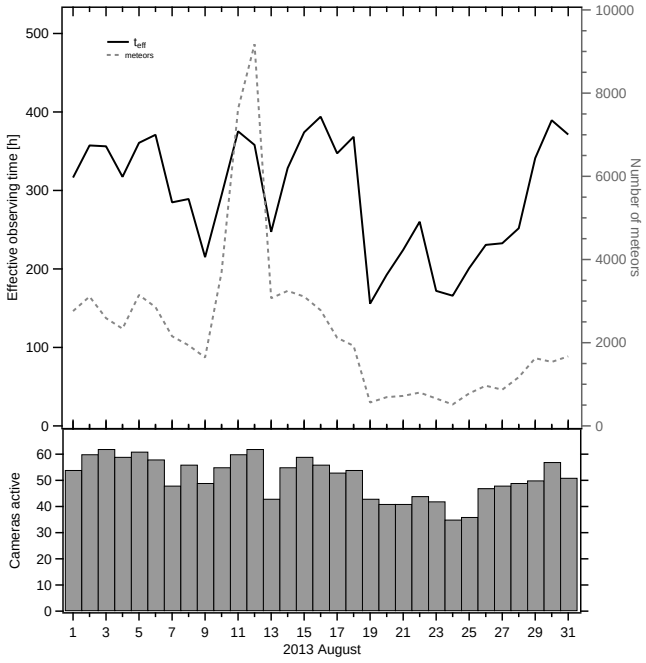

Figure 1 – Monthly summary for the effective observing time (solid black line), number of meteors (dashed gray line) and number of cameras active (bars) in 2013 August.

2 Perseids

Highlight of August were the Perseids just as every year. Figure 2 shows the flux density profile from the week around the maximum, composed from observations between 2011 and 2013. We are looking at a unique data set, because hardly any other shower can provide up to 10 000 meteor records in a single night. In total, almost 50 000 Perseids contributed to Figure 2. Each data point represents at least two hours, hence it contains so many meteors that there is almost no scatter. At a zenith exponent of $r = 1.9$, the profiles of the individual years fit seamlessly to one another and yield a smooth graph, if we forget about a few outliers at the begin or end of a night. The activity profile teaches us that we missed the primary peak at 140° solar longitude in all three years. Whereas observation stopped

[1]Abenstalstr. 13b, 84072 Seysdorf, Germany. Email: sirko@molau.de
[2]Na Ajdov hrib 24, 2310 Slovenska Bistrica, Slovenia. Email: javor.kac@orion-drustvo.si
[3]Via Bobbio 9a/18, 16137 Genova, Italy. Email: stefano.crivello@libero.it
[4]via Umbria 21/d, 30037 Scorze (VE), Italy. Email: stom@iol.it
[5]University of Hertfordshire, Hatfield AL10 9AB, United Kingdom. Email: geert@barentsen.be
[6]Urbanizacao da Boavista, Lote 46, Linhaceira, 2305-114 Asseiceira, Tomar, Portugal. Email: rui.goncalves@ipt.pt

IMO bibcode WGN-416-molau-vidaug
NASA-ADS bibcode 2013JIMO...41..201M

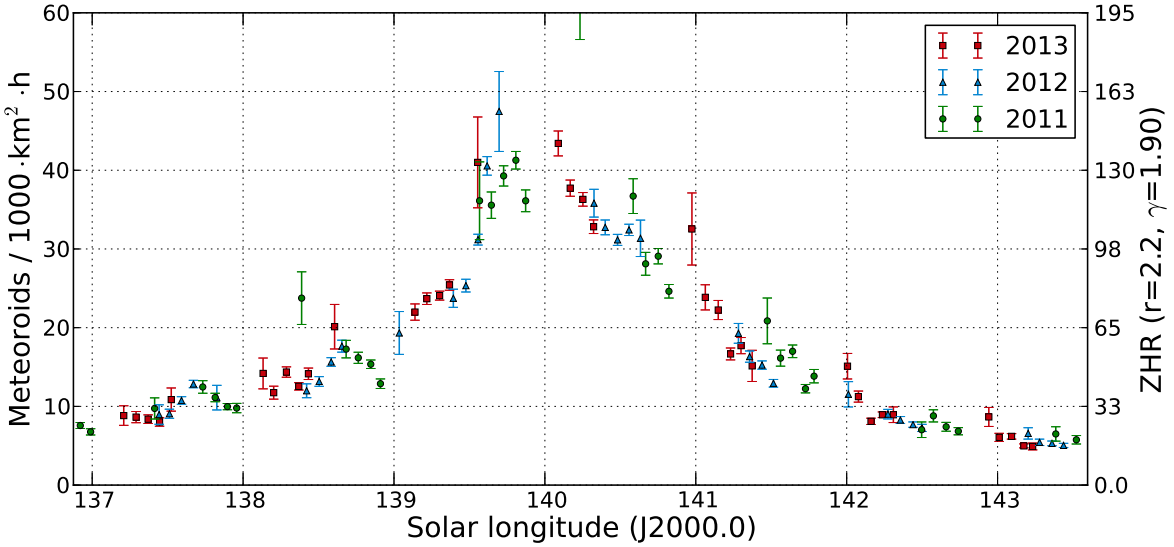

Figure 2 – Flux density profile of the Perseid peak in the years 2011 till 2013, obtained from almost 50 000 Perseids.

just before the peak in 2011, it started right after the peak in 2013. Thus, the main peak should be within the European night time hours of 2014.

3 Population index

At the last IMC, Jürgen Rendtel (2013) reminded us in his lecture to the importance of the population index r. The r-value describes the ratio between bright and faint meteors, or more specifically: How many more meteors there are up to magnitude class $m + 1$, compared to magnitude class m. If the limiting magnitude of the observer (or video system) is close to magnitude +6.5, the population index can be neglected, as it has virtually no impact on the ZHR or flux density. The stronger the limiting magnitude deviates from magnitude +6.5, however, the more important becomes the use of the proper r-value.

Video observations have one disadvantage and one advantage: The disadvantage is, that they cover a broad spectrum of limiting magnitudes. Due to different camera sensitivities and objective lenses, we obtain limiting magnitudes between roughly magnitudes +2 and +7 in the IMO Network. So the chosen population index has a major influence on the calculated flux density.

The advantage of video observations is the same fact, that they cover a broad spectrum of limiting magnitudes. This allows us to determine the population index with a completely new approach. Whereas current methods rely on the brightness distribution of meteors or at least their average brightness (relative to the limiting magnitude), our new approach does not need any meteor brightness measurements at all (which is good, because the photometry of meteors in MetRec is known to be quite inaccurate). But more about this new approach later on.

At first we shall analyze, how the population index impacts the flux density. Similar to visual quick look analyses, the MetRec Flux Viewer uses for each shower an average population index. The formula to calculate the flux density FD looks simplified as follows:

$$FD = MC \cos(ZD^{\gamma})/T_{\text{eff}}/\Sigma_{\text{pix}}(CA/r^{6.5-MLM}) \quad (1)$$

Here, MC is the meteor count, ZD the zenith distance of the radiant, γ the zenith exponent, T_{eff} the effective observing time (in hours), CA the collection area of a pixel (in km^2 at the meteor layer), r the population index and MLM the meteor limiting magnitude.

The formula contains two ingredients: There are the "global" parameters zenith distance, zenith exponent, meteor count and effective observing time, which are valid for the full field of view, and there are the "local" parameters collection area and meteor limiting magnitude, which vary from pixel to pixel. The last two parameters have to be calculated for each pixel individually and accumulated later on. The closer a pixel lies to the horizon, for example, the larger is the collection area at the meteor layer (roughly at 100 km altitude depending on the meteor shower velocity), but the more distant is the meteor layer.

Unfortunately, the population index is part of the term that has to be accumulated pixel-wise. Since the r-value is unknown at the time of observation, we would need to store the meteor limiting magnitude for each pixel at each minute to be able to adjust the flux density once the correct population index is known later on. As the cameras are unguided, the collection area of each pixel remains nearly constant in the course of the night, but the distance to the meteor shower radiant changes, and thereby the apparent meteor velocity and the resulting loss in limiting magnitude, too.

We have checked whether we find an approximation that requires the storage of fewer parameters. As first order approximation we assumed, that the meteor limiting magnitude would be constant in the field of view

($AVGMLM$). Then we can take this fixed term out of the sum and obtain:

$$FD \approx MC \cos(ZD^{\gamma})/T_{\mathrm{eff}}/r^{6.5-AVGMLM}/\Sigma_{\mathrm{pix}}(CA) \quad (2)$$

If during the calculation of the flux density a population index x was assumed, and later on the correct value y was determined, the correction factor for the flux density CF_{xy} can be expressed as:

$$CF_{xy} = x^{6.5-AVGMLM}/y^{6.5-AVGMLM} \quad (3)$$

To evaluate how good or bad this approximation is, we used real observing data from Remo1 obtained on 2013 August 12/13 and 13/14. The first night was partly clouded and the limiting magnitude was changing heavily in the course of the night, whereas the second night was almost completely cloud-free. Figure 3 shows the effective collection area for active meteor showers in those two nights depending on the population index. A range of r between 1.5 and 3.5 was chosen. That is, for every minute, every pixel and every population index between 1.5 and 3.5 (in steps of 0.1), the collection area of the camera was calculated and accumulated over time. We see that the collection area varies up to a factor of ten if the population index changes strongly.

If the described approximation is applied, the graphs look similar. Thus, we do not present the absolute values in Figure 4, but rather the relative errors between the approximated and the original values from Figure 3.

For each shower, the relative error becomes zero at a different population index, as there were different initial r-values chosen. In the typical range for r-values, the error is less than 15% but in extreme cases it may become as big as 50%. The error is nearly independent of the observing conditions as can be seen when comparing both nights.

In the second order approximation we used the fact that the dependency between the collection area and the r-value (Figure 3) can be expressed by a power law function of the type: $CA = ar^b$.

If the collection area is summed up independently for each r-value in the course of the night, we can later estimate the parameters a and b of a power law function that describes the dependency of the collection area (resp. flux density) from the population index. In Figure 5, we compare the values derived by this improved approximation with the original values from Figure 3. The error has reduced by one order of magnitude in this example. In extreme cases (poor observing conditions, strong deviation of the population index) it may reach 5% – under real conditions it is hardly ever larger than 2%.

Finally the approach was improved once more by computing the power law function not from the collection area accumulated over the full night, but individually for each minute of observation (Figure 6). This way, the relative error can be reduced by roughly a factor of three again. In the example of Remo1, it was 1.5% at most (independent of the observing conditions,

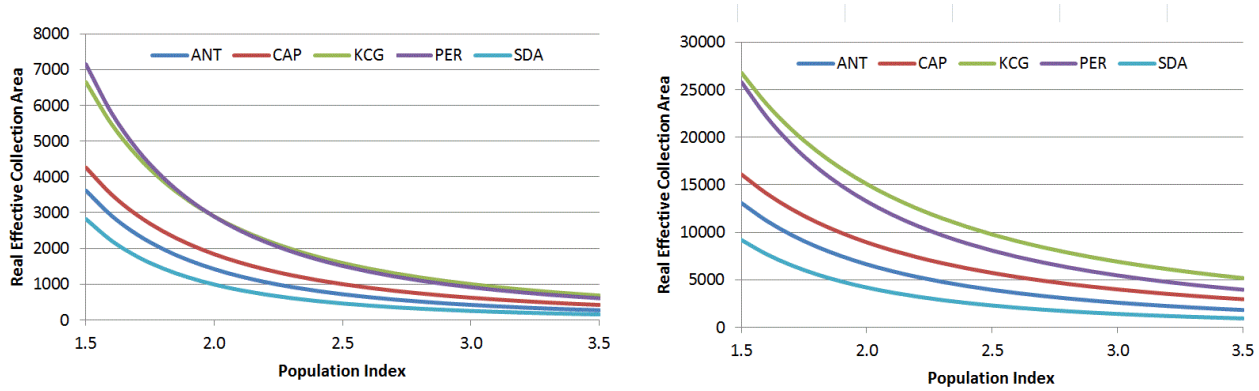

Figure 3 – Effective collection area of Remo1 for different meteor showers on 2013 August 12/13 (left) and 13/14 (right) depending on the population index.

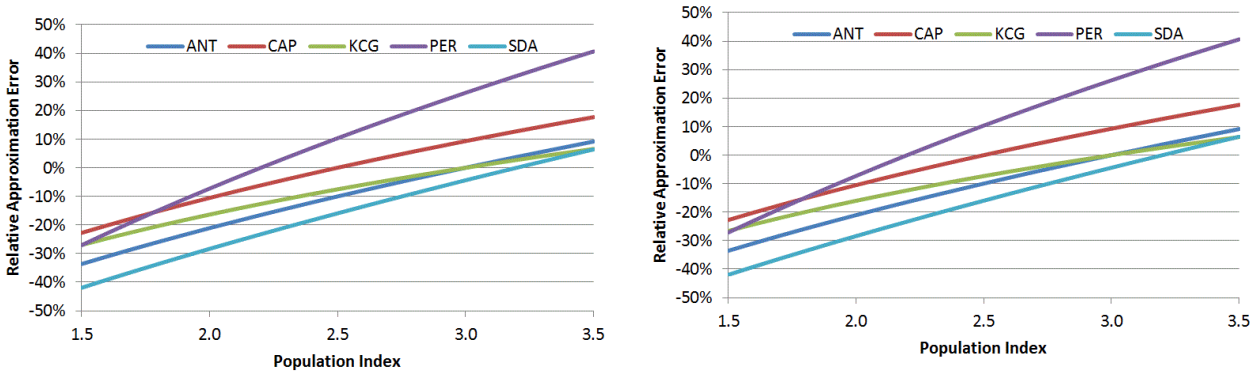

Figure 4 – Relative approximation error, if the pixel-wise limiting meteor magnitude is replaced by an averaged value. Calculated for the data of Remo1 on 2013 August 12/13 (left) and 13/14 (right).

Figure 5 – Relative approximation error, when the dependency of the collection area from the population index is approximated by a power law function. Calculated for the data of Remo1 on 2013 August 12/13 (left) and 13/14 (right).

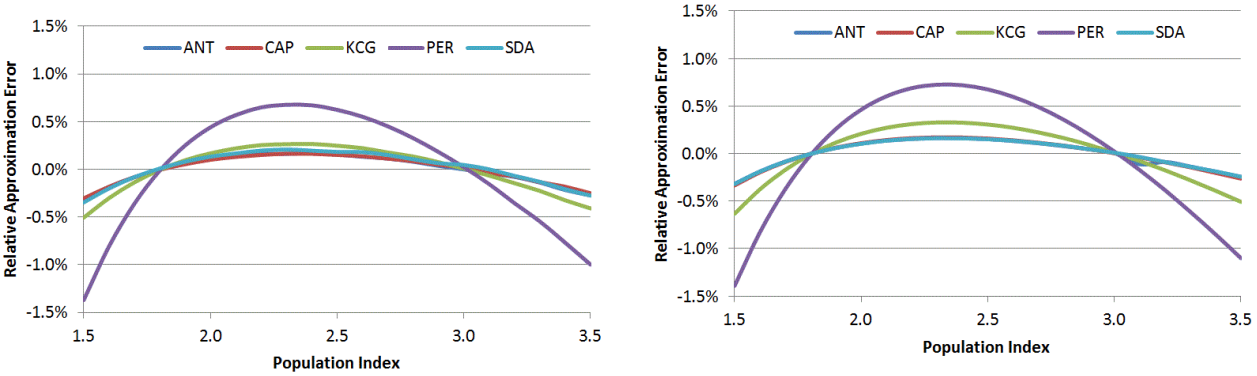

Figure 6 – Relative approximation error,when the dependency of the collection area from the population index is approximated by a power law function every minute. Calculated for the data of Remo1 on 2013 August 12/13 (left) and 13/14 (right).

because the fit is calculated for each minute individually), and less than half a percent for typical deviations of the population index. This error is clearly smaller than other rounding and systematic errors which are introduced during the calculation of the flux density (e.g. when the stellar limiting magnitude is calculated over the full field of view).

What does that mean in practice? As before, MetRec calculates for every minute the limiting magnitude and the effective collection area of all pixels, however, not just for the average shower-dependent population index, but rather for different r-values between 1.5 and 3.5. With a least squares algorithm, the parameters a and b of a power law function are determined such that the dependency of the collection area (and thereby also flux density) is approximated. If the flux density was determined with the initial population index x, but shall be adjusted later for the correct r-value y, the correction factor CF_{xy} becomes: $CF_{xy} = x^b/y^b$.

The scaling factor a of the power law function can even be omitted, because it can be derived easily when both the collection area and the exponent b are stored. So every minute, MetRec computes beside the current parameters like the limiting magnitude, collection area and radiant altitude an additional exponent b. It allows for the precise correction of the collection area resp. flux density once the proper population index is known.

Let us finally come back to our new approach on the calculation of the population index without knowing the meteor brightness or brightness distribution. Each camera "samples" the meteor population at a different limiting magnitude. Via the approximation described above we can calculate for each camera, how the flux density depends on the population index. Based on data sets of different cameras we simply have to determine that r-value at which the flux densities of the different cameras match best to one another!

Even though the correction function x^b/y^b looks trivial at the first glimpse, we did not find a closed-form solution for the optimization problem. So in practice we plan to determine the best population index by an iterative approximation. The procedure requires that there are no camera-dependent properties which systematically influence the flux density. So whether the r-values determined by our new approach are really useful has still to be shown in practice.

References

Molau S., Kac J., Berko E., Crivello S., Stomeo E., Igaz A., and Barentsen G. (2012). "Results of the IMO Video Meteor Network – August 2012". *WGN, Journal of the IMO*, **40:6**, 201–206.

Rendtel J. (2013). "From rates to fluxes". In *Proceedings of the International Meteor Conference, Poznan, Poland, 22-25 August 2013.* (to appear).

Handling Editor: Javor Kac

Table 1 – Observers contributing to 2013 August data of the IMO Video Meteor Network. Eff.CA designates the effective collection area.

Code	Name	Place	Camera	FOV [°²]	Stellar LM [mag]	Eff.CA [km²]	Nights	Time [h]	Meteors
BANPE	Bánfalvi	Zalaegerszeg/HU	Huvcse01 (0.95/5)	2423	3.4	361	19	97.7	557
BERER	Berkó	Ludányhalászi/HU	Hulud1 (0.8/3.8)	5542	4.8	3847	24	143.1	2413
			Hulud2 (0.95/4)	3398	3.8	671	22	140.4	829
			Hulud3 (0.95/4)	4357	3.8	876	24	139.6	518
BIRSZ	Biro	Agostyán/HU	Huago (0.75/4.5)	2427	4.4	1036	27	150.3	848
BOMMA	Bombardini	Faenza/IT	Mario (1.2/4.0)	5794	3.3	739	30	169.0	2155
BREMA	Breukers	Hengelo/NL	Mbb3 (0.75/6)	2399	4.2	699	14	74.6	504
			Mbb4 (0.8/8)	1470	5.1	1208	25	135.2	566
BRIBE	Klemt	Herne/DE	Hermine (0.8/6)	2374	4.2	678	27	149.1	744
		Bergisch Gladbach/DE	Klemoi (0.8/6)	2286	4.6	1080	28	135.4	836
CRIST	Crivello	Valbrevenna/IT	Bilbo (0.8/3.8)	5458	4.2	1772	31	200.1	1988
			C3P8 (0.8/3.8)	5455	4.2	1586	30	188.0	1499
			Stg38 (0.8/3.8)	5614	4.4	2007	31	203.7	2241
DONJE	Donani	Faenza/IT	Jenni (1.2/4)	5886	3.9	1222	24	142.1	1909
ELTMA	Eltri	Venezia/IT	Met38 (0.8/3.8)	5631	4.3	2151	27	172.3	1611
GONRU	Goncalves	Tomar/PT	Templar1 (0.8/6)	2179	5.3	1842	31	233.5	1165
			Templar2 (0.8/6)	2080	5.0	1508	30	234.2	1327
			Templar3 (0.8/8)	1438	4.3	571	31	225.9	967
			Templar4 (0.8/3.8)	4475	3.0	442	28	220.0	1437
GOVMI	Govedič	Središče ob Dravi/SI	Orion2 (0.8/8)	1447	5.5	1841	28	153.0	1273
			Orion3 (0.95/5)	2665	4.9	2069	23	124.4	649
			Orion4 (0.95/5)	2662	4.3	1043	27	141.0	852
HINWO	Hinz	Brannenburg/DE	Acr (2.0/35)*	557	7.3	5002	19	74.5	571
IGAAN	Igaz	Baja/HU	Hubaj (0.8/3.8)	5552	2.8	403	26	78.4	321
		Debrecen/HU	Hudeb (0.8/3.8)	5522	3.2	620	27	170.4	1251
		Hódmezővásárhely/HU	Huhod (0.8/3.8)	5502	3.4	764	29	136.0	828
		Budapest/HU	Hupol (1.2/4)	3790	3.3	475	25	128.0	378
KACJA	Kac	Ljubljana/SI	Orion1 (0.8/8)	1402	3.8	331	20	82.2	437
		Kamnik/SI	Cvetka (0.8/3.8)*	4914	4.3	1842	15	109.8	1544
			Rezika (0.8/6)	2270	4.4	840	16	108.0	1654
			Stefka (0.8/3.8)	5471	2.8	379	16	103.0	1288
		Kostanjevec/SI	Metka (0.8/12)*	715	6.4	640	12	91.1	650
KOSDE	Koschny	Izana Obs./ES	Icc7 (0.85/25)*	714	5.9	1464	20	176.7	1484
		La Palma/ES	Icc9 (0.85/25)*	683	6.7	2951	26	177.7	2494
		Noordwijkerhout/NL	Lic4 (1.4/50)*	2027	6.0	4509	20	101.7	810

Table 1 – Observers contributing to 2013 August data of the IMO Video Meteor Network – continued from previous page.

Code	Name	Place	Camera	FOV [°²]	Stellar LM [mag]	Eff.CA [km²]	Nights	Time [h]	Meteors
MACMA	Maciejewski	Chelm/PL	Pav35 (1.2/4)	4383	2.5	253	29	165.2	729
			Pav36 (1.2/4)*	5732	2.2	227	28	177.2	1107
			Pav43 (0.95/3.75)*	2544	2.7	176	27	155.5	528
MARGR	Maravelias	Lofoupoli-Crete/GR	Loomecon (0.8/12)	738	6.3	2698	21	147.3	871
MASMI	Maslov	Novosibirsk/RU	Nowatec (0.8/3.8)	5574	3.6	773	4	13.4	111
MOLSI	Molau	Seysdorf/DE	Avis2 (1.4/50)*	1230	6.9	6152	11	51.2	1059
			Mincam1 (0.8/8)	1477	4.9	1084	26	134.1	671
		Ketzür/DE	Remo1 (0.8/8)	1467	5.9	2837	31	158.5	1761
			Remo2 (0.8/8)	1478	6.3	4467	30	158.0	1171
			Remo3 (0.8/8)	1420	5.6	1967	31	149.0	442
MORJO	Morvai	Fülöpszállás/HU	Huful (1.4/5)	2522	3.5	532	30	167.3	916
OTTMI	Otte	Pearl City/US	Orie1 (1.4/5.7)	3837	3.8	460	22	89.0	645
PERZS	Perkó	Becsehely/HU	Hubec (0.8/3.8)*	5498	2.9	460	14	88.4	1336
PUCRC	Pucer	Nova vas nad Dragonjo/SI	Mobcam1 (0.75/6)	2398	5.3	2976	17	106.7	1213
ROTEC	Rothenberg	Berlin/DE	Armefa (0.8/6)	2366	4.5	911	11	46.0	298
SARAN	Saraiva	Carnaxide/PT	Ro1 (0.75/6)	2362	3.7	381	26	182.4	762
			Ro2 (0.75/6)	2381	3.8	459	28	224.3	1059
			Sofia (0.8/12)	738	5.3	907	25	194.9	672
SCALE	Scarpa	Alberoni/IT	Leo (1.2/4.5)*	4152	4.5	2052	27	143.6	1185
SCHHA	Schremmer	Niederkrüchten/DE	Doraemon (0.8/3.8)	4900	3.0	409	28	131.8	860
SLAST	Slavec	Ljubljana/SI	Kayak1 (1.8/28)	563	6.2	1294	22	130.7	413
STOEN	Stomeo	Scorze/IT	Min38 (0.8/3.8)	5566	4.8	3270	30	172.0	2337
			Noa38 (0.8/3.8)	5609	4.2	1911	29	172.5	2135
			Sco38 (0.8/3.8)	5598	4.8	3306	29	170.4	2425
STORO	Štork	Kunžak/CZ	Kun1 (1.4/50)*	1913	5.4	2778	4	23.3	821
		Ondřejov/CZ	Ond1 (1.4/50)*	2195	5.8	4595	5	31.7	1353
STRJO	Strunk	Herford/DE	Mincam2 (0.8/6)	2362	4.6	1152	25	110.5	475
			Mincam3 (0.8/6)	2338	4.5	1199	29	111.1	879
			Mincam4 (1.0/2.6)	9791	2.7	552	21	57.3	352
			Mincam5 (0.8/6)	2349	5.0	1896	26	129.6	798
TEPIS	Tepliczky	Budapest/HU	Humob (0.8/6)	2388	4.8	1607	26	146.0	1284
YRJIL	Yrjölä	Kuusankoski/FI	Finexcam (0.8/6)	2337	5.5	3574	24	94.5	589
						Overall	31	9 143.5	71 855

* active field of view smaller than video frame

Results of the IMO Video Meteor Network — September 2013

Sirko Molau[1], *Javor Kac*[2], *Stefano Crivello*[3], *Enrico Stomeo*[4], *Geert Barentsen*[5] *and Rui Goncalves*[6]

Preliminary results for September 2013 are presented of the IMO Video Meteor Network data, obtained by 69 cameras of the Network. More than 36 000 meteors were recorded in over 8 100 hours of effective observing time. A short-lived outburst of the September ε-Perseids was observed, with a maximum on 2013 September 9 at $22^{\mathrm{h}}00^{\mathrm{m}}$ UT. A detailed activity profile is presented for the outburst. A new procedure for population index was applied for the shower, yielding a population index value of 1.35.

Received 2013 November 28

1 Introduction

September 2013 was a mediocre month for the IMO Video Meteor Network. Whereas at first the perfect weather conditions of August continued, there were larger gaps in the observing statistics after the middle and in particular at the end of the month. Still, 41 out of the 69 active video cameras managed to obtain observations in 20 or more nights, which is a good result. Compared to last year (Molau et al., 2012b), the overall effective observing time was reduced by 10% to 8 100 hours, but the number of meteors increased by 10% to over 36 000 (Table 1 and Figure 1).

2 September ε- Perseids

The highlight of the month was the unexpected outburst of the September ε-Perseids (208 SPE) in the European evening hours of September 9. It was first mentioned by Japanese radio observers on the IMO-News mailing list, and only a short time later confirmed by video and visual observers from different European countries. The peak became soon visible in the MetRec flux viewer. However, different observers pointed out that the radiant position used by MetRec deviated clearly from the observed position.

Hence, the first analysis step was to determine the radiant position from all observations of 2013 September 9/10. 345 out of the 1302 meteors recorded during that night originated from a narrow radiant at $\alpha = 48\,^{\circ}\!.0$ / $\delta = 39\,^{\circ}\!.0$ with a standard deviation of $1\,^{\circ}\!.2$. The velocity was determined to be $v_{geo} = 65$ km/s. This radiant is just one degree off the position given in the IMO Meteor Shower Calendar (McBeath, 2012), and fits also nicely with the values obtained in our recent meteor shower analysis for the September ε-Perseids ($\alpha = 47\,^{\circ}\!.9$ / $\delta = 39\,^{\circ}\!.7$ / $v_{geo} = 64.5$ km/s at $\lambda_{\odot} = 167\,^{\circ}\!.2$).

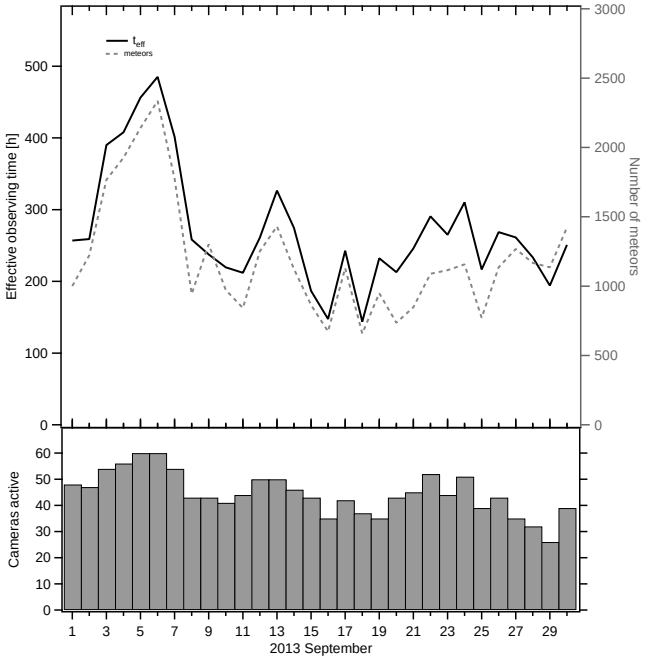

Figure 1 – Monthly summary for the effective observing time (solid black line), number of meteors (dashed gray line) and number of cameras active (bars) in 2013 September.

Based on these values, the shower assignment of the meteors was recomputed for all cameras. Indeed the SPE number almost doubled, because the previously used radiant position came from old tables. The corrected flux density data were uploaded to the MetRec flux viewer. Based on 288 shower meteors, the activity profile in Figure 2 was obtained.

At first glimpse, the short duration of the outburst is eye-catching. At $21^{\mathrm{h}}30^{\mathrm{m}}$ UT activity was still at the normal level. Half an hour later the outburst reached the peak, and after two hours the show was already over. As we recorded plenty of shower meteors in such a short period of time, we could calculate the activity profile at a high temporal resolution of 5 minutes just as was done for the Draconid outburst in 2011 (Molau et al., 2012a).

To determine the time of the maximum, we tested different parameter sets. According to these tests, the peak occurred exactly at $22^{\mathrm{h}}00^{\mathrm{m}} \pm 5^{\mathrm{m}}$ UT at a solar longitude $\lambda_{\odot} = 167\,^{\circ}\!.188$. That is later than the last known outburst of 2008, which was observed between $\lambda_{\odot}166\,^{\circ}\!.894$ and $166\,^{\circ}\!.921$ (McBeath, 2012).

[1]Abenstalstr. 13b, 84072 Seysdorf, Germany. Email: sirko@molau.de
[2]Na Ajdov hrib 24, 2310 Slovenska Bistrica, Slovenia. Email: javor.kac@orion-drustvo.si
[3]Via Bobbio 9a/18, 16137 Genova, Italy. Email: stefano.crivello@libero.it
[4]via Umbria 21/d, 30037 Scorze (VE), Italy. Email: stom@iol.it
[5]University of Hertfordshire, Hatfield AL10 9AB, United Kingdom. Email: geert@barentsen.be
[6]Urbanizacao da Boavista, Lote 46, Linhaceira, 2305-114 Asseiceira, Tomar, Portugal. Email: rui.goncalves@ipt.pt

IMO bibcode WGN-416-molau-vidsep
NASA-ADS bibcode 2013JIMO...41..207M

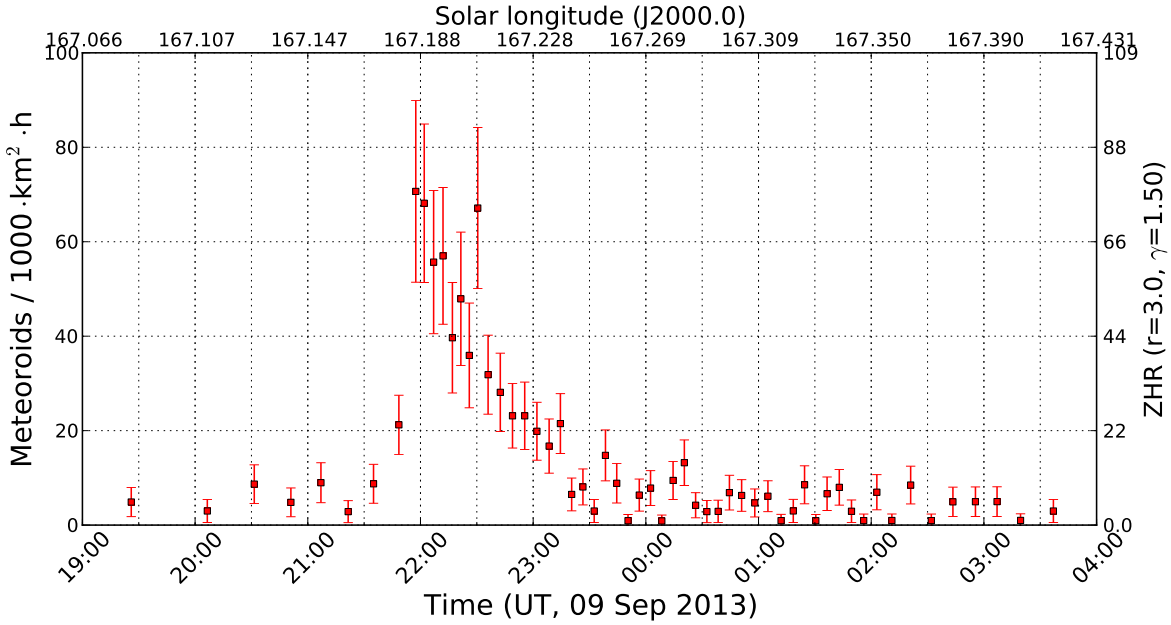

Figure 2 – Flux density profile of the September ε-Perseids on 2013 September 9/10, calculated with a standard population index of 3.0. In reality the population index was much smaller.

It is also remarkable that the brief ascending branch contains almost no data points, whereas the longer descending branch is well represented. The reason is not a lack of observations before $22^{\mathrm{h}}00^{\mathrm{m}}$ UT, but rather that there were indeed almost no shower meteors recorded at that time. The September ε-Perseids showed up literally instantaneously and declined a little slower.

To substantiate these qualitative statements with figures, we fitted a higher order polynomial to both the ascending and descending branches and determined to most important points in time. If the background activity is defined as 10 meteoroids per 1 000 km^2 per hour, the outburst started at $21^{\mathrm{h}}40^{\mathrm{m}}$ UT ($\lambda_\odot = 167\overset{\circ}{.}175$) and reached half-maximum at $21^{\mathrm{h}}49^{\mathrm{m}}$ UT ($\lambda_\odot = 167\overset{\circ}{.}181$). After the peak at $22^{\mathrm{h}}00^{\mathrm{m}}$ UT ($\lambda_\odot = 167\overset{\circ}{.}188$) the activity had dropped to half by $22^{\mathrm{h}}30^{\mathrm{m}}$ UT ($\lambda_\odot = 167\overset{\circ}{.}209$) and back to the background level at $23^{\mathrm{h}}30^{\mathrm{m}}$ UT ($\lambda_\odot = 167\overset{\circ}{.}249$). That yields a full width at half maximum (FWHM) of just 41 minutes or $0\overset{\circ}{.}028$ in solar longitude – roughly half of the Draconids 2011 duration.

At the descending branch we see a single outlier at $22^{\mathrm{h}}30^{\mathrm{m}}$ UT ($\lambda_\odot = 167\overset{\circ}{.}209$). However, depending on the parameter set this peak is sometimes really prominent and sometimes almost invisible, which is why its reality is questionable.

The absolute value of the peak flux density depends mainly on two parameters – the zenith exponent γ and the population index r. A zenith exponent of $\gamma = 1.0$ yields a maximum of about 50 meteoroids per 1 000 km^2 per hour, at $\gamma = 2.0$ it is already 90. The analysis presented by us at the 2012 IMC (Molau & Barentsen, 2013) derived zenith exponents between 1.5 and 2.0 for different showers. Hence, we obtain a peak value of 70 meteoroids per 1 000 km^2 per hour with a rather conservative value of $\gamma = 1.5$ and the standard population index of $r = 3.0$. Note that many observers reported that the outburst consisted mainly of bright meteors, so the population index must have been much smaller.

In our last monthly report we presented a method to determine the population index from data of different video cameras (Molau et al., 2013). That procedure was applied here for the first time. At first we selected cameras with mainly clear skies between $21^{\mathrm{h}}30^{\mathrm{m}}$ and $23^{\mathrm{h}}30^{\mathrm{m}}$ UT, because clouds may skew the limiting magnitude significantly. For this subset of cameras we determined the mean flux density of the September ε-Perseids in the two-hour period mentioned above depending on the population index. The result was plotted for all cameras in Figure 3.

We now look for the population index r at which the flux density measures of all cameras agrees best, i.e. when the scatter of the individual value is lowest. Naturally, the standard deviation σ reduces automatically the smaller the mean μ becomes. For this reason we used a "relative standard deviation" σ/μ as criterion. Furthermore, Figure 3 is presented with a logarithmic scale so that the scatter in the data is also proportional to the mean. Three cameras that clearly deviated from the average value were regarded as outliers and removed from the analysis.

Subjectively, the set of curves seem to be densest at r-values slightly below 1.5. That fits to the "relative standard deviation" which was lowest at $r = 1.35$. That population index is extremely small, but in the end it reflects the visual appearance and the results of individual cameras: Most September ε-Perseids were recorded by systems like Bilbo, Met38, Noa38 and Sco38, which have a large field of view but a poor limiting magnitude for this shower's meteors of +1 to +2 magnitude only. Cameras like Avis2 and Icc9 with smaller fields of view and a higher SPE limiting magnitude around +5 magnitude, on the other hand, recorded almost no shower members. The percentage of bright

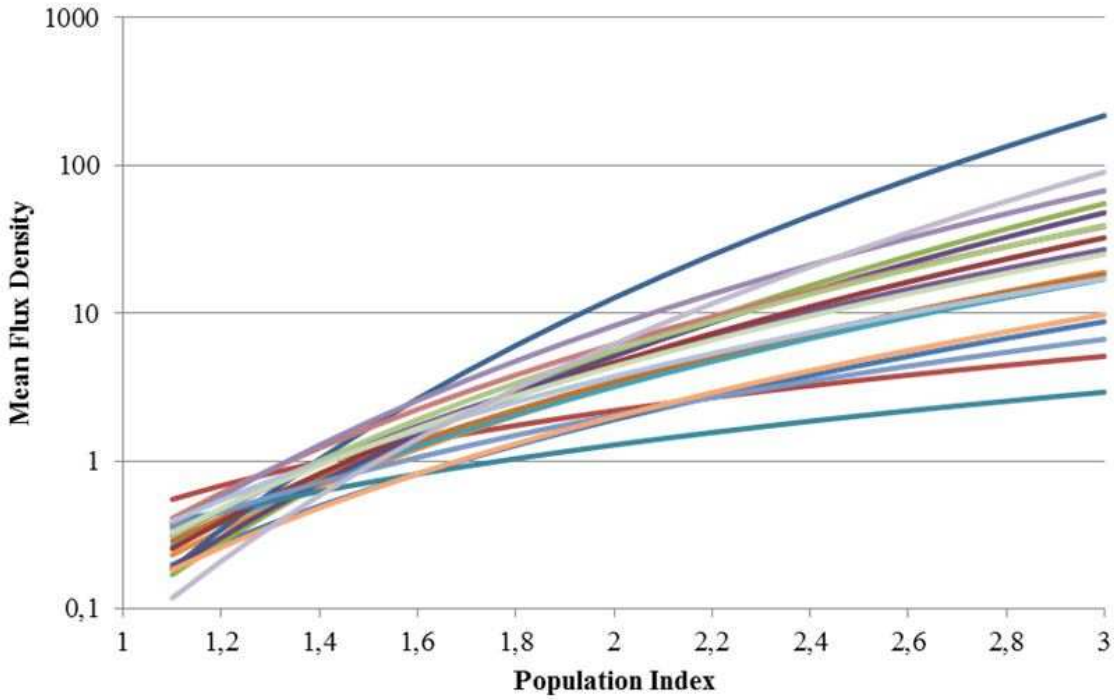

Figure 3 – Mean flux density of individual cameras between 21^h30^m and 23^h30^m UT depending on the chosen population index. The log of the flux density is plotted to represent the relative deviation of the measurements.

meteors, which can be observed best with a wide angle camera, was over-proportionally high.

At the assumed population index of $r = 1.35$, the flux density reduces to less than 2% of the value at $r = 3.0$. If this population index is correct, the above-mentioned peak flux density would be reduced to an almost negligible 1.3 meteoroids per 1 000 km^2 per hour. We are curious what r-value is derived from visual observations and how our new procedure for the determination of the population index performs under less exotic conditions.

References

McBeath A. (2012). "2013 Meteor Shower Calendar". International Meteor Organization. IMO INFO(2-12).

Molau S. and Barentsen G. (2013). "Meteoroid stream flux densities and the zenith exponent". In Gyssens M. and Roggemans P., editors, *Proceedings of the International Meteor Conference, La Palma, Canary Islands, Spain, 20–23 September 2012*. International Meteor Organization, pages 11–17.

Molau S., Kac J., Berko E., Crivello S., Stomeo E., Igaz A., and Barentsen G. (2012a). "Results of the IMO Video Meteor Network – October 2011". *WGN, Journal of the IMO*, **40:1**, 41–47.

Molau S., Kac J., Berko E., Crivello S., Stomeo E., Igaz A., and Barentsen G. (2012b). "Results of the IMO Video Meteor Network – September 2012". *WGN, Journal of the IMO*, **40:6**, 207–212.

Molau S., Kac J., Crivello S., Stomeo E., Barentsen G., and Goncalves R. (2013). "Results of the IMO Video Meteor Network – August 2013". *WGN, Journal of the IMO*, **41:6**, 201–206.

Handling Editor: Javor Kac

Table 1 – Observers contributing to 2013 September data of the IMO Video Meteor Network. Eff.CA designates the effective collection area.

Code	Name	Place	Camera	FOV [°²]	Stellar LM [mag]	Eff.CA [km²]	Nights	Time [h]	Meteors
ARLRA	Arlt	Ludwigsfelde/DE	Ludwig1 (0.8/8)	1488	4.8	726	6	50.7	52
BANPE	Bánfalvi	Zalaegerszeg/HU	Huvcse01 (0.95/5)	2423	3.4	361	14	47.2	125
BASLU	Bastiaens	Hove/BE	Urania1 (0.8/3.8)*	4545	2.5	237	7	33.2	45
BERER	Berkó	Ludányhalászi/HU	Hulud1 (0.8/3.8)	5542	4.8	3847	17	120.0	929
			Hulud2 (0.95/4)	3398	3.8	671	14	111.6	303
			Hulud3 (0.95/4)	4357	3.8	876	13	102.4	142
BOMMA	Bombardini	Faenza/IT	Mario (1.2/4.0)	5794	3.3	739	29	174.2	1266
BREMA	Breukers	Hengelo/NL	Mbb3 (0.75/6)	2399	4.2	699	18	91.3	304
			Mbb4 (0.8/8)	1470	5.1	1208	6	30.3	83
BRIBE	Klemt	Herne/DE	Hermine (0.8/6)	2374	4.2	678	21	111.6	451
		Bergisch Gladbach/DE	Klemoi (0.8/6)	2286	4.6	1080	20	90.6	444
CRIST	Crivello	Valbrevenna/IT	Bilbo (0.8/3.8)	5458	4.2	1772	27	178.0	706
			C3P8 (0.8/3.8)	5455	4.2	1586	25	163.4	556
			Stg38 (0.8/3.8)	5614	4.4	2007	26	182.0	973
DONJE	Donani	Faenza/IT	Jenni (1.2/4)	5886	3.9	1222	28	220.2	1409
ELTMA	Eltri	Venezia/IT	Met38 (0.8/3.8)	5631	4.3	2151	24	150.8	610
GONRU	Goncalves	Tomar/PT	Templar1 (0.8/6)	2179	5.3	1842	20	169.5	633
			Templar2 (0.8/6)	2080	5.0	1508	22	183.3	636
			Templar3 (0.8/8)	1438	4.3	571	26	182.7	512
			Templar4 (0.8/3.8)	4475	3.0	442	22	180.3	601
GOVMI	Govedič	Središče ob Dravi/SI	Orion2 (0.8/8)	1447	5.5	1841	21	118.2	451
			Orion3 (0.95/5)	2665	4.9	2069	17	99.5	182
			Orion4 (0.95/5)	2662	4.3	1043	15	87.9	209
HINWO	Hinz	Brannenburg/DE	Acr (2.0/35)*	557	7.3	5002	13	75.5	449
IGAAN	Igaz	Baja/HU	Hubaj (0.8/3.8)	5552	2.8	403	24	104.6	326
		Debrecen/HU	Hudeb (0.8/3.8)	5522	3.2	620	27	121.1	402
		Hódmezővásárhely/HU	Huhod (0.8/3.8)	5502	3.4	764	21	128.6	338
JONKA	Jonas	Budapest/HU	Husor (0.95/4)	2286	3.9	445	24	157.6	387
KACJA	Kac	Ljubljana/SI	Orion1 (0.8/8)	1402	3.8	331	17	70.2	148
		Kamnik/SI	Cvetka (0.8/3.8)*	4914	4.3	1842	15	66.3	287
			Rezika (0.8/6)	2270	4.4	840	15	73.1	408
			Stefka (0.8/3.8)	5471	2.8	379	18	83.0	275
		Kostanjevec/SI	Metka (0.8/12)*	715	6.4	640	3	19.1	68
KISSZ	Kiss	Sülysáp/HU	Husul (0.95/5)*	4295	3.0	355	27	129.5	141
KOSDE	Koschny	Izana Obs./ES	Icc7 (0.85/25)*	714	5.9	1464	28	243.0	2439
		La Palma/ES	Icc9 (0.85/25)*	683	6.7	2951	23	164.7	1928
		Noordwijkerhout/NL	Lic4 (1.4/50)*	2027	6.0	4509	21	103.1	685

Table 1 – Observers contributing to 2013 September data of the IMO Video Meteor Network – continued from previous page.

Code	Name	Place	Camera	FOV [°²]	Stellar LM [mag]	Eff.CA [km²]	Nights	Time [h]	Meteors
MACMA	Maciejewski	Chelm/PL	Pav35 (1.2/4)	4383	2.5	253	16	104.3	307
			Pav36 (1.2/4)*	5732	2.2	227	15	108.8	435
			Pav43 (0.95/3.75)*	2544	2.7	176	14	105.1	198
MARGR	Maravelias	Lofoupoli-Crete/GR	Loomecon (0.8/12)	738	6.3	2698	20	168.3	514
MASMI	Maslov	Novosibirsk/RU	Nowatec (0.8/3.8)	5574	3.6	773	14	74.7	597
MOLSI	Molau	Seysdorf/DE	Avis2 (1.4/50)*	1230	6.9	6152	20	101.4	1130
			Mincam1 (0.8/8)	1477	4.9	1084	25	117.1	308
		Ketzür/DE	Remo1 (0.8/8)	1467	5.9	2837	24	145.0	1439
			Remo2 (0.8/8)	1478	6.3	4467	23	145.6	918
			Remo3 (0.8/8)	1420	5.6	1967	21	137.4	215
MORJO	Morvai	Fülöpszállás/HU	Huful (1.4/5)	2522	3.5	532	23	136.4	327
OCHPA	Ochner	Albiano/IT	Albiano (1.2/4.5)	2944	3.5	358	1	3.4	21
OTTMI	Otte	Pearl City/US	Orie1 (1.4/5.7)	3837	3.8	460	26	191.2	795
PERZS	Perkó	Becsehely/HU	Hubec (0.8/3.8)*	5498	2.9	460	24	125.5	684
PUCRC	Pucer	Nova vas nad Dragonjo/SI	Mobcam1 (0.75/6)	2398	5.3	2976	17	80.3	398
ROTEC	Rothenberg	Berlin/DE	Armefa (0.8/6)	2366	4.5	911	15	90.3	234
SARAN	Saraiva	Carnaxide/PT	Ro1 (0.75/6)	2362	3.7	381	23	159.5	381
			Ro2 (0.75/6)	2381	3.8	459	23	184.6	398
			Sofia (0.8/12)	738	5.3	907	22	164.3	267
SCALE	Scarpa	Alberoni/IT	Leo (1.2/4.5)*	4152	4.5	2052	8	53.5	173
SCHHA	Schremmer	Niederkrüchten/DE	Doraemon (0.8/3.8)	4900	3.0	409	24	128.0	494
SLAST	Slavec	Ljubljana/SI	Kayak1 (1.8/28)	563	6.2	1294	17	65.8	121
STOEN	Stomeo	Scorze/IT	Min38 (0.8/3.8)	5566	4.8	3270	25	147.2	998
			Noa38 (0.8/3.8)	5609	4.2	1911	23	128.3	729
			Sco38 (0.8/3.8)	5598	4.8	3306	27	154.8	1064
STRJO	Strunk	Herford/DE	Mincam2 (0.8/6)	2362	4.6	1152	17	93.5	397
			Mincam3 (0.8/12)	2339	5.5	3590	20	95.6	577
			Mincam4 (1.0/2.6)	9791	2.7	552	1	9.7	30
			Mincam5 (0.8/6)	2349	5.0	1896	18	95.1	475
TEPIS	Tepliczky	Budapest/HU	Humob (0.8/6)	2388	4.8	1607	28	152.4	686
		Agostyán/HU	Huago (0.75/4.5)	2427	4.4	1036	25	158.8	520
YRJIL	Yrjölä	Kuusankoski/FI	Finexcam (0.8/6)	2337	5.5	3574	24	104.4	422
						Overall	30	8 148.6	36 155

* active field of view smaller than video frame

History

Meteor Beliefs Project: The tenth anniversary

Alastair McBeath[1]

An eclectic mixture of short items, some with an element of humour, concerning mostly meteoritic beliefs from texts and films, is presented to celebrate the Project's tenth anniversary, including material sent by contributors George Drobnock, John Naylor and Roy Watson. The Project's aims are reiterated, along with brief comments on future plans.

Received 2013 March 27

1 Introduction

When Andrei Gheorghe and I initially conceived the Meteor Beliefs Project in 2002, we did not foresee how it would have developed and grown since our inaugural article was published ten years ago (McBeath & Gheorghe, 2003). The response to the Project has been excellent, both in terms of the positive appreciation and interest shown to the published material, and in the contributions of fresh information and articles received for it. It has become clear too that some of the matters tackled have come to form an area of increasing importance for professional science researchers in recent years, helping to engage students in a way that "pure" science sometimes does not, and perhaps more valuably, because of a growing understanding that myth and folklore may contain real information about past unusual events. A couple of examples. The London Geological Society published "Myth and Geology" in early 2007 (Piccardi & Masse, 2007), noted as "the first peer-reviewed collection of papers focusing on the potential of myth storylines to yield data and lessons that are of value to the geological sciences." The book was based on papers presented to a conference held during 2004 in Italy, and included a somewhat less detailed review of several items we have already covered in the Project, such as many of the Classical Mediterranean period's meteoritic, or supposedly meteoritic, objects. International Year of Astronomy in 2009 enjoyed a strongly-promoted cultural element too. As noted in advance by Robson (2007), "The main aim of IYA2009 will be a global celebration of astronomy (in its very widest sense), including its contributions to society and culture, stimulating worldwide interest not only in astronomy, but in science in general, with a slant towards young people". That overall attitude seems to have persisted since in places, particularly when trying to better engage or retain a positive public perception of the subject.

Originally, much of this paper was intended to mark the Project's fifth anniversary in 2008, together with commemorating the centenary of the Tunguska event then. Although it was presented at that year's IMC with this aim, the article, in common with the Project's others so-presented, and for unknown reasons, was not published in that meeting's Proceedings volume. Thus it has been reworked here with minimal amendment, aside from in the first and final pairs of sections.

In preparing this piece, the Project's initial article was drawn upon for inspiration as to its format. Consequently, the Project's aims are reviewed, followed by a selection of shorter items, including those with a note of deliberate – sometimes accidental – humour, concentrating chiefly on meteoritic and impact-related events because of the intended Tunguska connection. As part of the process of taking stock at this anniversary, some things it is hoped may be examined in future are also briefly noted.

2 Project's aims

The Project's central concept remains as it began a quite simple one, but with far-reaching and open-ended potential. Anyone with information to share is invited to submit their favourite literary, poetic, mythological or folkloric references to meteors. These will then be either re-edited into compilation articles such as this one, if shorter items, or for longer pieces, presented in a suitable format for publication under the authorship of the originators and the Meteor Beliefs Project banner. Contributors are always acknowledged whichever is the case.

From time to time, details from fictional films and TV programmes (and any associated novels) are collected and published in a similar vein, under the "Meteoric Imagery in SF" sub-Project strand (on which see most recently McBeath & Gheorghe, 2012). A second additional strand, "Musical Meteors" collects and examines meteoric elements from contemporary song lyrics (see McBeath & Gheorghe, 2010), or indeed from instrumental pieces of music, where a particular meteoric connection was intended.

For anything sent-in, details must be provided as to exactly where the reference came from, giving as much information as possible, and including things such as specific line numbers for poems and plays, verse numbers for songs, or dates, places and people where oral tales were collected, for example. The information should be sufficient to allow any future investigator to easily find and confirm the report. An English translation is required for whatever is provided, but in some cases an original-language version may need to be pre-

[1]12a Prior's Walk, Morpeth, Northumberland, NE61 2RF, England, UK. Email: mcbal.gwyvre@virgin.net

IMO bibcode WGN-416-mcbeath-mbp-decenial
NASA-ADS bibcode 2013JIMO...41..212M

sented too (perhaps where poetic scansion cannot be properly represented in English). If there are particular problems with words or concepts that cannot be translated, these should be made clear. In uncertain cases, please make contact in advance to discuss the point.

There are no strong restrictions on what material the Project may collect and present, whether contemporary or past. However, a simple reference to a meteor being seen with no other embellishment is less useful than one which gave more description of the event, or which made some connection to, or comment on, how the event was perceived. The Project's purpose is to look at what people believed and believe about meteors, not necessarily what may be scientifically relevant (though the scientific view is of course just the latest beliefs about meteors, based on what evidence is believed acceptable at present!).

Constructive comments and ideas for anything linked to the Project are always welcomed. If you think something has been missed, or if you have found a variant translation that seems interesting, do say so. The Project's coordinators are far from infallible! If unsure, send the material anyway. Do not be concerned your report may duplicate someone else's. It would be preferable to receive some material that cannot be used, or several repetitions of the same thing, than miss the chance to bring to light some long-forgotten or potentially important item, for instance. In all cases, the Project is reliant upon you to help move it forwards!

3 Latter-day "stone rains"?

To begin, something to show one can never be sure where potentially interesting snippets may be found. In Section B, pp. 311–316 of Chapter 9 in (Safar et al., 1981), entitled "Geological Notes on Rocks, Fossils and Objects of Antiquarian Interest Excavated from the Ruins of Eridu", by W Rees Williams, and written in 1948, Specimen Number 35 on p. 315 was of note. It was a broken angular pebble of clear rock crystal quartz. This type of rock is found only in restricted places in Iraq modernly, none of them at all close to the ancient city of Eridu (whose earliest remains date to circa 5500 BC), now in the desert of southern Iraq, roughly 50 km southwest of Nasiriyah.

Williams went on to describe where a pebble of this kind could have originated: "One such area is found along the southern slopes of the mountains of Kurakazhaw and at places east of Barzinja, about 15 miles S.S.E. of Choarta. Here, water-clear, double ended crystals of quartz are picked up quite frequently after the snows melt or after rain. They have weathered out of the limestone and are washed out of the overlayer of soil. The local people believe that they have fallen from the skies like hail. These crystals are never more than 1 to 2 inches long."

Modern Chwarta is in the Iraqi Zagros Mountains east of Kirkuk, about 25 km (15 miles) north-northwest of modern Sulaymaniyah, near where the 2.5 to 5 cm crystals might be collected. Perhaps beliefs of this sort related to the portentous Classical "rains of stones", as noted most recently from Livy and Obsequens in the Project (Gheorghe & McBeath, 2006). Whether the twentieth-century-recorded tale was known in ancient Mesopotamia, and what influence it may have had on one of these gem-quality stones ending up in Eridu, around 550 km from Chwarta – if the stone came from there directly – remain unknown.

4 Wells' *Natural Philosophy* of 1857

Project contributor George Drobnock came across the following items from David A Wells' book *Natural Philosophy* (an 1859 university edition, the original text published in 1857), pp. 288–290, while carrying out some research into possible fossil meteorites in coal seams in his home state of Pennsylvania, USA. They gave an insight into beliefs about meteors and meteorites during the great years of discovery in the subject.

Wells' described: "Meteorites are luminous bodies, which from time to time appear in the atmosphere, moving with immense velocity, remaining visible but for a few moments. They are generally accompanied by a luminous train, and during their progress explosions are often heard."

He made the following points:

1. The height above the Earth's surface meteors appeared was 18 to 80 miles (around 30 to 130 km).
2. Their entry velocity was 300 miles per minute ($\sim$ 8 km/s). He cited that one meteor flew within 25 miles of the Earth ($\sim$ 40 km) at a rate of 1200 miles per minute ($\sim$ 32 km/s).
3. An aerolite (that is, a meteorite) possessed a black, shiny crust, which when broken open was of a grey colour.
4. A meteorite consisted of iron and nickel with other substances.
5. Meteorites were found in South Africa, Mexico, Siberia and overland on the route to California. As George commented, this latter point is particularly interesting given that the Californian gold-rush began in 1849, which saw tens of thousands of people heading west across America, many of them with at least some metallurgical knowledge, only eight years before Wells' book was first published.

Finally, Wells offered the following hypotheses for meteors and meteorites:

1. Rocks thrown up by terrestrial volcanoes falling back to Earth.
2. Meteors were produced in the atmosphere by vapours and gases.
3. Meteors entered the atmosphere from lunar volcanoes.
4. Meteors were of the same nature as the planets, either derived from them, or existing independently.

He concluded that he was in favour of the fourth and third of these hypotheses.

5 Kazantsev's *Flaming Island* of 1959

More than twenty years ago, then-budding atmospheric optics author John Naylor contacted me about various naked-eye astronomical topics, and a series of detailed discussions followed. John's book was finally published in 2002 (Naylor, 2002), but during those earlier discussions, John kindly provided some notes and copies from the second volume of a text by American astronomer Nicholas Bobrovnikoff (1990), published posthumously, as Bobrovnikoff had died in 1988. Bobrovnikoff's work contained the reference to Kazantsev's novel used here. Bobrovnikoff's own pioneering work in correlating asteroid spectral reflectivities with those of meteorites during the 1920s and 30s was covered briefly, with references, by (Bowden, 2006, pp. 390–391), for example.

On pages 205–206 of his text, Bobrovnikoff began with a discussion of the antimatter hypothesis for the 1908 Tunguska event, pointing out the flaws in it, and why it was unnecessary to explain the observed phenomena. He then went on to comment on the novels of popular Russian author A P Kazantsev, who had written several books centred around what he believed had occurred at Tunguska. As Bobrovnikoff put it, Kazantsev's science-fiction "is actually pure fiction, without any appreciable scientific content in it." He then provided the following synopsis of the 1959 novel *Flaming Island*:

"...in which the Tunguska episode is explained as an invasion from Mars in which the Martian ship is blown up in the atmosphere of the earth. Only one female scientist is saved from the [c]atastrophe and she gives the hero a piece of extremely heavy metal, "radium-δ," which is a source of inexhaustible energy. Further developments are purely political, with the wicked capitalists nearly ruining the world by starting an uncontrollable atomic reaction on the Flaming Island, which turns out to be a gigantic meteorite. As usual in such Soviet morality plays, the virtuous communists save humanity, this time by using the piece of radium-δ from Mars."

So now Tunguska has been "explained" as due to an exploding craft from both Venus (McBeath & Gheorghe, 2006, pp. 59–60) and Mars during the Meteor Beliefs Project!

6 Kendrick's *A Fire in the Sky* of 1978

Long-standing Project contributor Roy Watson provided the next item, another science-fiction novel, this time by Walter Kendrick (1978). Roy noted that this was basically a story about a comet on a collision course with Earth, and the two astronomers who attempted to alert the public as to its predicted impact site – Phoenix, Arizona – against the wishes of politicians. Some of the passages Roy felt were of especial interest concentrated around the comet's impact.

Page 155: "As it neared the ground, the comet grew larger than the sun and a thousand times brighter. The noise was beyond human endurance, and Phoenix was silhouetted like a toy town against the glow of a fire from the sky. When the comet's head sank below the horizon, there was a moment of silence – total, ominous silence – before beams of incredible light came shooting up from its impact point like God's own fireworks. For an instant, light pulsed and beamed, then all was blotted out by a white and yellow fireball that bloomed like a cosmic flower across the heavens. Then sound caught up with light, and Phoenix shook to its foundations."

Page 159: "Seen from as far away as Tucson, the comet made a spectacle that could be called beautiful because from there, there was no danger. A long white streak, beginning to diffuse like a vapour trail, cut across the distant sky, breaking off thousands of feet above the ground, where the comet had entered the earth's atmosphere. It made a sort of cosmic arrow pointing towards Phoenix."

As too often with the meteoric phenomena we have found portrayed in fiction, physical laws become little more than loose guidelines to be ignored in favour of dramatic effect whenever desired. Tucson is roughly 175 km from Phoenix in Arizona, so in reality, its "safety" would have been relative and short-lived, while the "thousands of feet" to where the comet entered the atmosphere should have been at least "hundreds of thousands" (e.g. 120 km $\simeq$ 400 000 feet). Time for some comedic cartoon-style running away from Tucson, perhaps!

7 *Evolution* (colour film, 2001)

Among the movies which did not make it onto the initial listing for the "Meteoric Imagery in SF" strand (given in McBeath & Gheorghe, 2005) were several where the meteoric elements were of interest, but relatively too slight to warrant an in-depth examination, including the three films discussed below.

Evolution, directed by Ivan Reitman, was a comic action movie in the loose mould of one of his earlier successes *Ghostbusters*. It was the tale of two unconventional college professors Ira Kane (played by TV's *X-Files* star David Duchovny) and Harry Bloch (Orlando Jones), who had to battle a rapidly-evolving alien invader, which arrived on Earth aboard a small meteoritic asteroid.

The movie opened with a shot of an "asteroid" looking as if it was made of mica-rich slate – angular, with laminated layers, and sparkling surfaces – approaching the Earth. It emitted contrail-like jets as if it was really slightly cometary. As it started to glow in the atmosphere, it made a whooshing sound, and after beginning to fragment, broke up with the noise of a soft explosion, followed by fizzing and crackling noises, a little like a fire, leaving a thin trail of smoke.

Cutting to the view from Earth, a bright spot appeared high up in the sky which grew larger (but oddly not much brighter), emitting a flaming trail. With a whooshing sound, this blazing "meteor", trailing smoke, smashed at quite high (though well below natural meteoric) velocity into a shack, around 40 or 50 metres behind a man running away from it. The whole erupted in a quite modest explosion, knocking the man flat, while throwing his car, parked a little nearer the shack, high

into the air. The aftermath was a smoking crater where the shack had been, with scattered small fires on the ground nearby.

Naturally, this was done for dramatic, and to an extent comic, effect, though whether the lay-audience would appreciate the differences to a real cosmic velocity impact seemed unlikely. The fact it was set in the "Meteor Crater" state of the USA, Arizona, was obviously intended to lend a crude note of "realism" to the plot (as presumably also with the Kendrick novel discussed above).

The two professors from a local community college went out to investigate next day, albeit Orlando Jones' geologist character was provided with only a sketchy knowledge of his supposed subject, and insisted on calling the impactor "a meteor". The fallen object had made a crater around 5 m wide (the scale was almost impossible to judge on-screen, however), and had punched a hole down into a cavern about 25 m below. In this cavern was a ~ 4 m-across piece of the "sparkly slate" meteorite, partly buried in the floor, smoking still, and hot to the touch, but already with extraterrestrial nitrogen-based organisms growing and rapidly evolving on its surface.

Various return visits to the cave found the object had created its own subterranean ecosystem of increasingly complex lifeforms. Attempts to halt the process met with failure, until it was realised selenium was deadly to the creatures. This resulted in the comically-intended use of the anti-dandruff shampoo "Head & Shoulders" to combat the alien invasion, because it contained selenium!

The whole was handled entertainingly enough, and there was no real pretence at seriousness in any of it, other than for temporary dramatic effect. Even the use of selenium, an element whose name derives from *Selene* = "the Moon", had its own mildly amusing undertone, particularly as the Moon is often used in metaphorical ways for things insane or illusory. One of the better deliberately humorous approaches to the use of meteorites in films overall.

8 *Lara Croft – Tomb Raider* (colour film, 2001)

Unsurprisingly for a film based on a computer game, the plot, such as it was, was transparently thin, but the whole moved along well enough under the direction of Simon West, and was helped by a lively, dynamic performance of the eponymous heroine's role by Angelina Jolie. The meteoritic aspects of the story included the centrally important halves of a metal triangle made from a "meteor" (as the characters called it) that had fallen to Earth 5000 years earlier. The huge crater the original meteorite created was set in Siberian Russia, shown in the film as a vast circular lake with a central ring of mountains, called either "The Ice Lake" or "Meteor Crater Lake", and was obviously so-located to take advantage of the unmentioned real-world knowledge of the Tunguska event.

The lake had obstacles such as icebergs to be avoided (**that** large a lake!), while the central island was ice-covered, and could be crossed only by dog sled, as modern technology like engines and computers refused to work within the "dead zone" ringed by the implausibly huge, jagged peaks. The triangular artefact had been created in a city built inside this crater, but misuse of its more or less magical "otherworldly" powers had caused the city's destruction in ancient times. The object was split in two so this could not be repeated, or at least, not until the storyline required it. Disaster was of course avoided by an unlikely hairsbreadth at the film's climax, during an equally improbable once-in-5000-years planetary conjunction (including all the, as they were then nine, planets) and a solar eclipse where the dark circle of the lunar disc was helpfully visible beyond the eclipsed Sun!

9 *Ring of the Niebelungs* (colour film, 2004)

This German movie, directed by Uli Edel, was a variant retelling of the great Norse-Germanic tragedy concerning the legendary life of the hero Sigurd (German Siegfried), as detailed most fully in the Norse *Völsunga Saga* or the Germanic *Niebelungenlied*, although it is now perhaps better-known from the monumental operatic Ring Cycle of German composer Richard Wagner, begun in 1853. Information from and references to the earlier Norse versions can be traced via the name-entries in (Orchard, 1997), for instance – e.g. Sigurd, pp. 143–146.

From Project coordinator Andrei Gheorghe's viewing of it, the film had a number of differences to any of the earlier versions, but was still presented on a grand scale, and was just as dramatically effective. In most versions, Brynhild (Brunehilde) was a Valkyrie, one of the warrior-maidens who chose those killed in battle for a place of special honour in the afterlife, and when Sigurd first encountered her, she was magically asleep on the top of a mountain ringed by fire. Only Sigurd was brave enough to pass through the flames and awaken her. In the movie however, Siegfried (here a prince) and Brunehilde (Queen of Iceland) were brought together as they had both witnessed the fall of a spectacular, gigantic, meteoric fireball to Earth. The fireball had been cast down as a sign of the gods' fury. The pair arrived simultaneously from different directions at the crater this impact had left. From the meteoritic iron he found there, Siegfried forged a sword with which he later killed a dragon that had appeared nearby, and gained the Niebelungs' treasure the dragon had hoarded, which in turn set off the next stage of the tragedy, as the Niebelungs cursed him for his theft, and so on. This innovative segment partly reversed the commoner order from the Norse and German texts, where Sigurd/Siegfried usually had his magical sword made first, then killed the dragon, before going on to rescue Brynhild. The newer version had its own points of interest though, along with the meteoritic aspects, and is worth seeing complete.

10 Future plans for the Project

Among the materials currently in preparation are further items from the "Meteoric Imagery in SF" strand, and additional pieces from medieval European and more recent Native American meteor beliefs to complement those discussions already published. Some details of Maori beliefs from New Zealand are in progress too, although southern hemisphere meteor beliefs away from Oceania, particularly those from South America and Africa, have continued to prove unexpectedly elusive. Any fresh assistance with either area would be most welcome.

11 Conclusion

It is clear from correspondence and personal contacts that the Project has so far provided much of appeal to significant numbers of IMO members, and those beyond the Organization too, in giving back something of the more human, emotional, response to meteoric phenomena. It has also helped point out some of the misrepresentations or misinterpretations of matters meteoric and meteoritic that continue to feature in mainstream societal thought, and even sometimes in works by scientific authors who have strayed too far into meteoric myths and beliefs with insufficient knowledge. I hope that with your help, we can continue to do so. For now, I wish to conclude with grateful thanks to all those earlier authors who recorded the beliefs the Project has reported, and most especially to everyone who has provided the additional notes or complete articles used in the Project to date.

References

Bobrovnikoff N. T., editor (1990). *Astronomy Before the Telescope, Volume 2, The Solar System*. Pachart Publishing House.

Bowden A. J. (2006). "Meteorite provenance and the asteroid connection". In McCall G. J. H., Bowden A. J., and Howarth R. J., editors, *The History of Meteorites and Key Meteorite Collections: Fireballs, Falls and Finds*, London. Geological Society, pages 379–403.

Gheorghe A. D. and McBeath A. (2006). "Meteor Beliefs Project: Meteoric portents from Livy and Julius Obsequens". *WGN, Journal of the IMO*, **34:3**, 94–100.

Kendrick W. (1978). *A Fire in the Sky*. Tempo Star.

McBeath A. and Gheorghe A. D. (2003). "Meteor Beliefs Project: Introduction". *WGN, Journal of the IMO*, **31:2**, 55–58.

McBeath A. and Gheorghe A. D. (2005). "Meteor Beliefs Project: Meteoric Imagery in SF, Part I – Introduction". *WGN, Journal of the IMO*, **33:6**, 165–166.

McBeath A. and Gheorghe A. D. (2006). "Meteor Beliefs Project: Meteoric Imagery in SF, Part III – A Third Anniversary entertainment". *WGN, Journal of the IMO*, **34:2**, 58–60.

McBeath A. and Gheorghe A. D. (2010). "Meteor Beliefs Project: Musical Meteors, meteoric imagery as used in near-contemporary song lyrics". In Andreić Ž. and Kac J., editors, *Proceedings of the IMC, Poreč, 2009*. IMO, pages 95–99.

McBeath A. and Gheorghe A. D. (2012). "Meteor Beliefs Project: Meteoric Imagery in SF, Part VI – A brief history of impact movies, 1906–1999". *WGN, Journal of the IMO*, **40:6**, 213–220.

Naylor J. (2002). *Out of the Blue: A 24-hour Skywatcher's Guide*. Cambridge University Press.

Orchard A. (1997). *Dictionary of Norse Myth and Legend*. Cassell.

Piccardi L. and Masse W. B., editors (2007). *Myth and Geology (Special Publications 273)*. Geological Society, London.

Robson I. (2007). "International Year of Astronomy 2009". *A & G*, **48:4**, 4.30.

Safar F., Mustafa M. A., and Lloyd S., editors (1981). *Eridu*. Ministry of Culture & Information, State Organization of Antiquities and Heritage, Baghdad.

Handling Editor: Javor Kac
This paper has been typeset from a LaTeX file prepared by the author.

The International Meteor Organization

web site http://www.imo.net

Council

President: Jürgen Rendtel,
Eschenweg 16, D-14476 Marquardt, Germany.
tel. +49 33208 50753
e-mail: jrendtel@aip.de

Vice-President Cis Verbeeck,
Bogaertsheide 5, 2560 Kessel, Belgium.
e-mail: cis.verbeeck@scarlet.be

Secretary-General: Robert Lunsford
1828 Cobblecreek Street, Chula Vista,
CA 91913-3917, USA. tel. +1 619 585 9642
e-mail: lunro.imo.usa@cox.net

Treasurer: Marc Gyssens, Heerbaan 74,
B-2530 Boechout, Belgium.
e-mail: marc.gyssens@uhasselt.be
BIC: GEBABEBB
IBAN: BE30 0014 7327 5911
Always state BIC and IBAN codes together!
Check international transfer charges with your bank; you are responsible for paying these.

Other Council members:
Rainer Arlt, Bahnstr. 11, D-14974 Ludwigsfelde, Germany. e-mail: rarlt@aip.de
David Asher, Armagh Observatory, College Hill, Armagh, Northern Ireland BT61 9DG, UK.
e-mail: dja@arm.ac.uk
Geert Barentsen, University of Hertfordshire, Hatfield AL10 9AB, UK. e-mail: geert@barentsen.be
Javor Kac (see details under WGN)
Detlef Koschny, Zeestraat 46,
NL-2211 XH Noordwijkerhout, Netherlands.
e-mail: detlef.koschny@esa.int
Sirko Molau, Abenstalstraße 13b, D-84072 Seysdorf, Germany. e-mail: sirko@molau.de
Paul Roggemans (see details under IMC Liaison Officer)

Commission Directors

FIreball DAta Center: André Knöfel
Am Observatorium 2,
D-15848 Lindenberg, Germany.
e-mail: fidac@imo.net
Photographic Commission: vacant
Radio Commission: Jean-Louis Rault
Société Astronomique de France,
16, rue de la Vallée,
91360 Epinay sur Orge, France.
email: f6agr@orange.fr
Telescopic Commission: Malcolm Currie
660, N'Aohoku Place, Hilo, HI 96720, USA
e-mail: mjc@star.rl.ac.uk
Video Commission: Sirko Molau
Visual Commission: Rainer Arlt

IMC Liaison Officer

Paul Roggemans, Pijnboomstraat 25, 2800 Mechelen, Belgium, email: paul.roggemans@gmail.com

WGN

Editor-in-chief: Javor Kac
Na Ajdov hrib 24, SI-2310 Slovenska Bistrica, Slovenia. e-mail: wgn@imo.net;
include METEOR in the e-mail subject line
Editorial board: Ž. Andreić, R. Arlt, D.J. Asher, J. Correira, M. Gyssens, H.V. Hendrix, C. Hergenrother, J. Rendtel, J.-L. Rault, P. Roggemans, C. Trayner, C. Verbeeck.
Advisory board: M. Beech, P. Brown, M. Currie, M. de Lignie, W.G. Elford, R.L. Hawkes, D.W. Hughes, J. Jones, C. Keay, G.W. Kronk, R.H. McNaught, P. Pravec, G. Spalding, M. Šimek, I. Williams.

IMO Sales

Available from the Treasurer or the Electronic Shop on the IMO Website	€	$
IMO membership, including subscription to WGN Vol. 41 (2013)		
Surface mail	26	39
Air Mail (outside Europe only)	49	69
Electronic subscription only	21	29
Back issues of WGN on paper (price per complete volume)		
Vols. 26 (1998) – 35 (2007) except 30 (2002), 38 (2010) – 40 (2012)	15	23
Vols. 37 (2009) – 40 (2012) – electronic version only	9	13
Proceedings of the International Meteor Conference on paper		
1990, 1991, 1993, 1995, 1996, 1999, 2000, 2002, 2003, per year	9	13
2007, 2010, 2011, per year	15	23
2012	25	37
Proceedings of the Meteor Orbit Determination Workshop 2006	15	23
Handbook for Meteor Observers	20	29
Electronic media		
Meteor Beliefs Project CD-ROM	6	9
DVD: WGN Vols. 6–30 & IMC 1991, 1993–96, 2001–04	45	69

Bright fireball on 2013 October 30 over The Netherlands

This bright fireball was captured on 2013 October 30 at $03^{h}35^{m}$ UT by several cameras in The Netherlands and neighbouring countries. See front cover for a colour reproduction of the bottom-right photo, and pages 184 and 199 for some CAMS results.

CAMS 362 Alphen aan de Rijn, NL
Courtesy of Robert Haas

CAMS 361 Alphen aan de Rijn, NL
Courtesy of Robert Haas

Hengelo, NL
Courtesy of Martin Breukers

EN95 Benningbroek, NL
Courtesy of Jos Nijland